Journal Pre-proof

Proxy VAR models in a data-rich environment

Martin Bruns

PII: S0165-1889(20)30214-1
DOI: https://doi.org/10.1016/j.jedc.2020.104046
Reference: DYNCON 104046

To appear in: *Journal of Economic Dynamics & Control*

Received date: 23 July 2020
Revised date: 11 November 2020
Accepted date: 20 November 2020

Please cite this article as: Martin Bruns, Proxy VAR models in a data-rich environment, *Journal of Economic Dynamics & Control* (2020), doi: https://doi.org/10.1016/j.jedc.2020.104046

Proxy VAR models in a data-rich environment

Martin Bruns*

December 5, 2020

Abstract

I propose a Bayesian approach to identify vector autoregressive (VAR) models via proxies in a data-rich environment. The setup augments a small-scale VAR model with latent factors. It allows to trace out the responses of disaggregated series in a unified model while controlling for broad economic conditions. The posterior sampler accounts for the estimation uncertainty in these latent factors as well as the measurement precision of the proxy. In a first application to monetary policy, I extract factors from a wide range of real and financial series and find that the effects of monetary policy shocks vary along the yield curve. In a second application to oil market shocks I add disaggregated US series to a standard model of the global oil market. I find that negative news about future oil supply have adverse effects on the US economy.

JEL classification: C38, E60

Keywords: Factor-augmented VAR, external instruments, structural VAR, monetary policy, oil market shocks

*University of East Anglia. Email: martin.bruns@uea.ac.uk. I am grateful to Lutz Kilian, Helmut Lütkepohl, Haroon Mumtaz, Michele Piffer, Barbara Rossi, and two anonymous referees for their valuable suggestions. Participants at the T2M conference, the Royal Economic Society Annual Meeting, the European Economic Association Annual Meeting, the Econometric Society Winter Meeting and the ASSA meeting provided helpful comments. I thank the German Academic Scholarship Foundation for financial support. An early version of this project circulated under the name "Combining Factor Models and External Instruments to Identify Uncertainty Shocks".

1 Introduction

Proxy vector-autoregressive (Proxy-VAR) models are widely used to study the dynamic impact of structural shocks on the economy. Their popularity stems from the fact that they avoid the use of potentially non-credible timing restrictions implicit in conventional recursive identification schemes. However, typical Proxy-VAR models include only a small number of variables. This has two potential disadvantages: First, it is difficult to examine the impact of structural shocks at a disaggregated level in a single, unified model. Second, broad economic concepts need to be measured using individual, often narrowly defined, variables. These considerations motivate a transition to a data-rich environment.

A natural approach to summarise the information in rich datasets is provided by factor-augmented VAR (FAVAR) models. FAVAR models augment small-scale VARs with latent factors extracted from a large number of series. In so doing, they allow for a disaggregated analysis in a single, unified model. At the same time, FAVARs offer a way of controlling for abstract economic concepts such as "output", "price level", or "financial conditions". They avoid having to associate these concepts to single, somewhat arbitrarily-chosen data-series. Instead, the approach employs information from a large number of series related to these concepts, e.g. financial spreads with different maturities, and summarises their joint behaviour in latent factors.

The first contribution of this paper is to propose a Bayesian Proxy Factor-augmented VAR (BP-FAVAR) model. This model offers a unified framework to combine a rich dataset with an identification strategy based on a proxy. It extends the approach proposed by Caldara and Herbst (2019) to allow for latent factors and accounts for their estimation uncertainty in a consistent Bayesian framework. The second contribution of the paper is to investigate the properties of the BP-FAVAR in a simulation exercise and in two applications for which the inclusion of factors is particularly natural and for which proxies are available.

The first application investigates the effects of monetary policy shocks. Caldara and Herbst (2019) revisit the question of which variables central banks' policy decisions were based on during the Great Moderation in a small-scale Proxy VAR model. They rely on a high-frequency identification scheme and make the observation that central banks base their policy decisions not just on deviations of output, unemployment and inflation from their targets but also on financial conditions. In order to measure financial conditions, Caldara and Herbst (2019) include a corporate bond yield spread, the

Baa spread, as an additional variable.[1] They show that when including this variable, monetary policy shocks have large and persistent effects on real activity and prices. However, Baa-rated debt accounts for less than half of total corporate debt, making the Baa spread a potentially too narrow measure of financial tightness.[2] This narrow definition could potentially lead to the model being non-fundamental for the shock of interest and restricts the analysis of the effects of monetary policy to this measure. Therefore, the inclusion of a broader measure of financial conditions is warranted. This need for a broader measure of financial conditions (and other economic concepts) leads me to transition to the framework by Bernanke et al. (2005) using a single observable factor, the policy rate, and extract factors from a large number of informational series, avoiding the need to measure abstract economic concepts using narrowly-defined variables. I exploit the BP-FAVAR model setup to investigate the reaction of financial spreads with different maturities to monetary policy shocks. I find that monetary policy shocks have an effect that varies substantially across the yield curve, especially in the the medium run.

I then apply the model to oil market shocks. I revisit Känzig (2019) who proposes a new proxy to investigate the effects of shocks in the global oil market on the US economy. Employing a small-scale Proxy VAR model, the author identifies oil supply news shocks in the global oil market and makes the observation that oil supply news shocks differ from conventional oil supply shocks in their effect on oil inventories. He then traces out the reactions of various US variables by estimating separate small-scale Proxy VAR models including various US variables of interest. This procedure omits cross-correlations among these US variables given that they enter in distinct models. For this reason, instead of estimating various distinct models, I propose to model the US variables jointly in the BP-FAVAR by adding latent factors from a large number of US series to an otherwise standard VAR model of the global oil market. I investigate the reactions of various US variables to the identified oil supply news shocks. I qualitatively confirm the findings in Känzig (2019) about the adverse effects of negative news about future oil supply on US industrial production and unemployment rate. In addition, the data-rich BP-FAVAR allows to conclude that, consistent with economic intuition, the subcomponent of US industrial production related to fuel is most strongly affected and

[1] They employ Moody's seasoned Baa corporate bond yield relative to the yield on 10-year treasury constant maturity.

[2] In 2018, 303 firms were rated Baa, issuing 41% of total debt of rated companies. See https://www.moodys.com/research/Moodys-Baa-rated-companies-nearly-double-in-the-decade-to–PBC_1171751.

that US stock markets drop and rebound following an adverse oil supply news shock.

This study relates firstly to Bayesian FAVAR models such as Bernanke et al. (2005) who introduce the FAVAR model, Belviso and Milani (2006) who provide a structural interpretation of the latent factors, and Amir-Ahmadi and Uhlig (2015) who employ sign restrictions in FAVAR models. In addition, it broadly relates to early applications of Bayesian factor models such as Kose et al. (2003). Secondly, this study relates to the Bayesian Proxy VAR literature, most directly to the small-scale Bayesian Proxy VAR model by Caldara and Herbst (2019). Other studies employing external instruments in the Bayesian paradigm are Drautzburg (2016) who estimates a narrative DSGE-VAR model, Bahaj (2020) who applies high-frequency identification in a multi-country framework, and Arias et al. (2018) who propose a Proxy VAR framework amenable to an importance sampler. More generally, Stock and Watson (2012) combine factor models and proxies in a frequentist setting and Kerssenfischer (2019) investigates the relation between factor models and proxy identification. In parallel work to mine, Miescu and Mumtaz (2019) develop a Bayesian FAVAR model identified via a proxy and study its potential to address deficient information in small-scale models. Their model setup differs from mine along three main dimensions: First, they operate within a non-stationary factor model, while I employ data which are transformed to be stationary. Second, while I estimate latent factors using a Kalman filter, they use Principal Components (PC) analysis. Third, their focus is on the effect of latent factors on informational insufficieny issues of small-scale models. My focus is on an extension of the estimation algorithm, the choice of priors and a new posterior sampler. Mumtaz and Theophilopoulou (2019) apply a Baysian Proxy FAVAR to trace out the effects of UK monetary policy on disaggregated wealth inequality.

One challenge using factor-augmented VAR models is how to account for the estimation uncertainty of latent factors. This is technically challenging using bootstrap techniques in the popular frequentist approach of estimating factors via PC (see for example Yamamoto, 2019). In addition, there are no asymptotic results justifying the use of such techniques, as pointed out by Kilian and Lütkepohl (2017). To address this issue, I exploit the state-space representation of the model and employ the algorithm by Carter and Kohn (1994). This fully parametric approach treats the latent factors as random variables and samples from their posterior distribution. This procedure is included as an additional Gibbs step in the Metropolis-within-Gibbs sampler of Caldara and Herbst (2019).

The remainder of this paper is organised as follows: Section 2 introduces the model,

section 3 discusses the algorithm, priors, starting values, and a Monte Carlo exercise, section 4.1 shows the monetary policy application and section 4.2 discusses the oil market application. The last section concludes.

2 The Proxy FAVAR

In this section I introduce the Bayesian Proxy FAVAR model, which consists of three equations: The observation equation, the transition equation and the proxy equation. I then show how identification is achieved.

First, consider the observation equation, which shows how latent and observable factors map into informational series:

$$\boldsymbol{x}_t = \Lambda^f \boldsymbol{f}_t + \Lambda^z \boldsymbol{z}_t + \boldsymbol{\xi}_t \tag{1}$$

$$\boldsymbol{\xi}_t \sim N(\mathbf{0}, \Omega) \tag{2}$$

where $\boldsymbol{x}_t$ is a $N \times 1$ vector of observable series, $\boldsymbol{f}_t$ is a $R \times 1$ vector of latent factors, and $\boldsymbol{z}_t$ is a $K \times 1$ vector of observable factors. Importantly, $\boldsymbol{x}_t$ does not contain any of the observable factors in $\boldsymbol{z}_t$. Λ^f is a $N \times R$ matrix of factor loadings for latent factors and Λ^z is a $N \times K$ matrix of coefficients for the observable factors. $\boldsymbol{\xi}_t$ is a $N \times 1$ vector of idiosyncratic errors. In general, these idiosyncratic $\boldsymbol{\xi}_t$ can be serially correlated, i.e. $Cov(\boldsymbol{\xi}_t, \boldsymbol{\xi}_{t-1}) \neq 0$, but they are uncorrelated across series, i.e. $Var(\boldsymbol{\xi}_t) = \Omega$ is assumed to be diagonal.

The latent factors $\boldsymbol{f_t}$ and the factor loadings Λ^f and Λ^z require additional normalisations. For the latent factors, I follow Stock and Watson (2016) in imposing the normalisation that $\Lambda^{f\prime}\Lambda^f = I$ and $Var(\boldsymbol{f_t})$ is diagonal with decreasing elements. For Λ^z I follow Bernanke et al. (2005) and impose that the upper $R \times K$ block is an zero matrix. These normalisations do not affect the space spanned jointly by the latent factors which is the object of interest in this study.

Next, consider the transition equation, which shows the dynamic evolution of the factors. It writes as a VAR(P) of the following form:

$$\boldsymbol{y}_t = \Pi \boldsymbol{w}_t + \boldsymbol{u}_t \tag{3}$$

$$\boldsymbol{u}_t \sim N(\mathbf{0}, \Sigma), \tag{4}$$

where $\boldsymbol{y}_t = \begin{bmatrix} \boldsymbol{f}_t \\ \boldsymbol{z}_t \end{bmatrix}$ stacks latent and observable factors in a vector. The coefficient matrix $\Pi = [\Pi_1, ..., \Pi_P]$ of dimension $(R+K) \times (P(R+K)+1)$ contains the autoregressive parameters of the VAR. $\boldsymbol{w}_t = [\mathbf{1}_{(R+K)\times 1}; \boldsymbol{y}_{t-1}, ..., \boldsymbol{y}_{t-P}]$ stacks a constant and P lags of $\boldsymbol{y}_t$. The $(R+K) \times 1$ vector of reduced form errors, $\boldsymbol{u}_t$, is serially uncorrelated, i.e. $Cov(\boldsymbol{u}_t, \boldsymbol{u}_{t-p}) = 0 \quad \forall t = 1, ..., T, \forall p = 1, ..., \infty$. $\boldsymbol{u}_t$ are uncorrelated with all leads and lags of the idiosyncratic errors, $\boldsymbol{\xi}_t$, i.e. $Cov(\boldsymbol{u}_t \boldsymbol{\xi}_{t-j}) = 0 \; \forall j, \forall t = 1, ..., T$.

I impose structure on the on-impact effects of structural shocks by assuming that the reduced form errors map into structural shocks as:

$$\boldsymbol{u}_t = B\boldsymbol{\epsilon}_t \tag{5}$$

$$\boldsymbol{\epsilon}_t \sim N(\mathbf{0}, I_{R+K}), \tag{6}$$

where B is a $(R+K) \times (R+K)$ matrix containing the on-impact effects of the structural shocks. Their variances are normalised to one, and they are contemporaneously uncorrelated. This implies the following relation between the reduced form covariance matrix and the matrix of on-impact effects: $\Sigma = BB'$

As is well known, further restrictions beyond those implied by the covariance matrix are needed to identify B. The reason is that the data cannot discriminate between observationally equivalent representations: All B such that $BB' = \Sigma$ yield the same likelihood.

In order to identify the first column of B, which I denote by $\boldsymbol{b}$, I augment the model by a "Proxy Equation", as in Caldara and Herbst (2019).[3] This equation shows the relation between structural shock and instrument and is given as:

$$m_t = \beta\epsilon_{1,t} + \sigma_\nu \nu_t \tag{7}$$

$$\nu_t \sim N(0, 1), \tag{8}$$

where m_t is a scalar instrument correlated with the shock of interest, $\epsilon_{1,t}$. The shock of interest is ordered first, without loss of generality. β captures the structural relationship between instrument and shock, while ν_t captures any noise contained in the instrument.

[3]Unlike their case, however, identification focuses on the on-impact effects of the shocks rather than on the contemporaneous relations of the variables included in the model. Put differently, the model imposes structure on B, rather than on B^{-1}. Caldara and Herbst (2019) estimate a so-called A-model (see Kilian and Lütkepohl, 2017 for a discussion). The A-model specification is appropriate given their aim of identifying a monetary policy equation. In the present context, however, interest lies on the on-impact effects of structural shocks.

The higher its variance, σ_ν^2, the less information the instrument contains about the shock of interest. Furthermore, m_t is contemporaneously uncorrelated with all other shocks, $\boldsymbol{\epsilon}_{-1,t}$, i.e. $E(m_t\boldsymbol{\epsilon}_{-1,t}) = 0\ \forall t$, where $\boldsymbol{\epsilon}_{-1,t}$ stands for a vector containing all but the first shock. In other words, the instrument needs to be both relevant and exogenous in order to be appropriate for identification. A further, implicit, assumption is that m_t is uncorrelated with leads and lags of all structural shocks, i.e. $E(m_t\boldsymbol{\epsilon}_{t+j}) = 0\ \forall j \neq 0$. For $j > 0$ this assumption is not restrictive given that structural shocks are defined as unexpected innovations to the process, as pointed out by Stock and Watson (2018). The absence of correlation with lags of the structural shocks (i.e. for $j < 0$) could in theory be relaxed by adding lags of $\boldsymbol{y}_t$ to the right-hand-side of (7). In addition, one could allow for auto-correlation in the instrument by adding lags of m_t. Neither extension would affect identification and, in line with Caldara and Herbst (2019), I restrict attention to the baseline case given in (7).

3 Bayesian Inference

The parameters of the BP-FAVAR model are estimated via a Metropolis-within-Gibbs sampler while the latent factors are drawn using the algorithm by Carter and Kohn (1994). In this section, I discuss the choice of priors and sketch an algorithm to generate draws from the posterior distribution.

3.1 Priors and Starting Values

Block 1: Observation Equation For the parameters of the observation equation, $\Lambda = [\Lambda^f \quad \Lambda^z]$ and Ω, I employ equation-by-equation normal-inverse Gamma priors of the form

$$\boldsymbol{\omega}_{ii} \sim IG(sc^*, sh^*) \tag{9}$$

$$\boldsymbol{\lambda}_i|\boldsymbol{\omega}_{ii} \sim N(\boldsymbol{\mu}^*_{\lambda,i}, \boldsymbol{\omega}_{ii}M_i^{*-1}), \tag{10}$$

where $\boldsymbol{\lambda}_i$ is the i-th row of Λ and $\boldsymbol{\omega}_{ii}$ is the i-th diagonal element of Ω. The prior parameters $sc^*, sh^*, \boldsymbol{\mu}^*_{\lambda,i}$, and M_i^{*-1} are chosen to imply diffuse priors (see Appendix A.2 for details). The algorithm starts from the Principal Components estimates for Λ and $F = [\boldsymbol{f}_1, ..., \boldsymbol{f}_T]$ and OLS-based estimates for Ω.

Block 2: Transition Equation Given a draw of factors, $\boldsymbol{y}_t$ follows a standard

$VAR(P)$ model. Therefore, one can employ a version of the Minnesota/ Litterman prior and specify independent normal-inverse Wishart priors:

$$vec(\Pi) \sim N(\boldsymbol{\mu}_{\Pi}^{*}, V_{\Pi}^{*}) \tag{11}$$

$$\Sigma \sim IW(S^{*}, \tau^{*}), \tag{12}$$

where $vec(\cdot)$ is the vectorisation operator that stacks the columns of a matrix one underneath the other into a vector. I set the prior mean for the autoregressive coefficients, $\boldsymbol{\mu}_{\Pi}^{*} = \mathbf{0}$, implying shrinkage towards white noise processes. This choice is motivated by the stationarity transformations of both $\boldsymbol{z}_t$ and $\boldsymbol{x}_t$. I set the prior variance of $vec(\Pi)$, V_{Π}^{*}, in line with Del Negro and Schorfheide (2011). Lastly, I set the priors $S^{*} = 0.0001 \cdot \boldsymbol{I_{K+R}}$ and $\tau^{*} = K + R$, implying a flat prior in the dimension of Σ (see Appendix A.3).

Block 3: Proxy Equation The parameters of the proxy equation are sampled conditional on the parameters of the transition equation and follow Caldara and Herbst (2019) closely. For β I employ a normal distribution

$$\beta \sim N(\mu_{\beta}^{*}, \sigma_{\beta}^{*2}) \tag{13}$$

with $\mu_{\beta}^{*} = 0$ and $\sigma_{\beta}^{*} = 1$.

For σ_{ν}^{2} I consider two types of priors: First, I set an uninformative inverse Gamma distribution using

$$\sigma_{\nu}^{2} \sim IG(sc_{\nu}^{*}, sh_{\nu}^{*}) \tag{14}$$

with $sc_{\nu}^{*} = 2$ and $sh_{\nu}^{*} = 0.02$. Second, to the extent that the econometrician is confident in the relevance of the proxy, she can employ what Caldara and Herbst (2019) refer to as the "high-relevance" prior and set

$$\sigma_{\nu} = 0.5 std(m_t), \tag{15}$$

implying the dogmatic view that half the standard deviation of the proxy (a quarter of the variance) can be explained by measurement error, while the remaining variation is explained by movements in the structural shock itself (see Appendix A.5).

The prior for $\boldsymbol{b}$ is implicit in the above priors on Σ, β and σ_{ν}.

3.2 Sketch of the Algorithm

Inference requires generating draws from the joint posterior distribution of latent factors and parameters given the informational series, the observable factors and the instrument:

$$p(\Pi, \Sigma, \Lambda^f, \Lambda^z, \Omega, \beta, \sigma_\nu, \boldsymbol{b}, F | X, Z, \boldsymbol{m}). \tag{16}$$

Instead of attempting to draw directly from this potentially highly non-linear and irregularly shaped distribution, draws are generated from blocks of conditional distributions in the following steps:

Step 1 **Draw from the conditional posterior of** F

In order to generate draws from

$$p(F | \Pi, \Sigma, \Lambda^f, \Lambda^z, \Omega, \beta, \sigma_\nu, \boldsymbol{b}; X, Z, \boldsymbol{m}), \tag{17}$$

I employ the Carter-Kohn algorithm described in Carter and Kohn (1994) and Frühwirth-Schnatter (1994) (see Appendix A.1).

Step 2 **Draw from the conditional posterior of** $\{\Lambda^f, \Lambda^z, \Omega\}$

To generate draws from

$$p(\Lambda^f, \Lambda^z, \Omega | F, \Pi, \Sigma, \beta, \sigma_\nu, \boldsymbol{b}; X, Z, \boldsymbol{m}), \tag{18}$$

one can exploit the fact that, given a draw of the latent factors, F, the observation equation (1) is a system of independent linear equations. Therefore, the parameters can be estimated using well-established results on single-equation models (see Appendix A.2).

Step 3 **Draw from the conditional posterior of** Π, Σ

To generate draws from

$$p(\Pi, \Sigma | \Lambda^f, \Lambda^z, \Omega, F, \beta, \sigma_\nu, X, Z, \boldsymbol{m}), \tag{19}$$

I employ a Metropolis-Hastings step. First, note that, conditional on a draw of the factors, the model can be considered a variant of Caldara and Herbst (2019). The conditional posterior in (19) differs from standard reduced form

Bayesian VAR models given that $\boldsymbol{m}$ is part of the conditioning set. To address this challenge, I proceed in two steps: First, I generate proposal draws from $p(\Pi, \Sigma|\Lambda^f, \Lambda^z, \Omega, F, \beta, \sigma_\nu, X, Z)$ ($\boldsymbol{m}$ is not part of the conditioning set) using well-established results on independent normal-inverse Wishart distributions. In a second step, these proposal draws are mapped into the target distribution (19) via a Metropolis-Hastings step (see Appendix A.4). In practice, the proposal distribution is highly similar to the target distribution, leading to an acceptance rate close to 1. This high acceptance rate does not imply a weak instrument, but rather indicates that the instrument does not contain much information about the reduced form parameters, a result also found in Caldara and Herbst (2019).

Step 4 **Draw from the conditional posterior of $\boldsymbol{b}$**

To generate draws from

$$p(\boldsymbol{b}|\Lambda^f, \Lambda^z, \Omega, F, \Pi, \Sigma, \beta, \sigma_\nu; X, Z, \boldsymbol{m}), \tag{20}$$

I use a second Metropolis-Hastings step, adapting the procedure by Caldara and Herbst (2019) to my setting. First, I generate proposal draws b^{cand} as the first column of $chol(\Sigma)Q^{cand}$, where Q^{cand} is an orthogonal matrix such that $Q^{cand}Q^{cand\prime} = I$. I then map this candidate draw into a draw from the target distribution (20) via a second Metropolis-Hastings step (see Appendix A.4).

Step 4 **Draw from the conditional posterior of β, σ_ν**

Lastly, to generate draws from

$$p(\beta, \sigma_\nu|\boldsymbol{b}, \Lambda^f, \Lambda^z, \Omega, F, \Pi, \Sigma; X, Z, \boldsymbol{m}) \tag{21}$$

I employ well-established results on linear regression models for the proxy equation (7). The structural shock can be generated as $\epsilon_{1,t} = chol(\Sigma)Q\boldsymbol{u}_t$.

Compared to the framework in Caldara and Herbst (2019), there are three main differences: First, the above approach includes latent factors and accounts for their estimation uncertainty in a consistent Bayesian setup, thereby allowing the factors to affect the dynamics of Z. Second, the BP-FAVAR allows for inference on a large number of potentially disaggregated series, X, through the mapping from factors to informational series. Third, this approach employs the proxy in order to identify the on-impact effects of structural shocks, $\boldsymbol{b}$, rather than the contemporaneous relations among variables, as

in Caldara and Herbst (2019). Further extensions, such as handling missing data, using multiple instruments for multiple shocks and/or multiple instruments for a single shock are in general feasible, but beyond the scope of this paper.

Compared to the common approach of replacing F by their Principal Components estimates (see Stock and Watson, 2016 for a review), this approach has two advantages: First, it captures the sampling uncertainty of factors within a coherent Bayesian framework, rather than treating them as observed data. Popular bootstrap inference as in Yamamoto (2019) is far from trivial and lacks asymptotic justification. A Bayesian approach, on the other hand, offers a unified way of summarising the uncertainty of the model, as pointed out by Huber and Fischer (2018). The joint posterior summarises estimation uncertainty in both the parameters and the latent factors. Second, this approach allows for Bayesian shrinkage of the parameter space of the transition equation. This might seem unnecessary given that the factors already reduce the dimensionality of the estimation problem. However, if, as is often the case in empirical applications, the number of observable factors, K, or the lag length, P, is large, dimensionality issues still arise and can be alleviated using Bayesian shrinkage.

3.3 Numerical Illustration

To verify the performance of the algorithm, this section presents a numerical illustration. Datasets are generated from a Proxy-FAVAR, an exercise similar in spirit to Lopes and West (2004). I generate 50 datasets, each containing 200 observations, a sample size commonly encountered in macroeconomic applications. 9 observational series are generated from a process with one lag, 3 latent factors, and one observable factor. The first data-generating process (DGP1) uses the first structural shock itself as a proxy for identification, while the second (DGP2) introduces some contamination in the proxy. This distinction is also used in Miescu and Mumtaz (2019). The details of both DGPs and additional results are presented in Appendix C.

Figure 1 shows the impulse responses of the informational series together with the true impulse response. Overall, the algorithm is well-centred around the true impulse response. Introducing measurement error in the proxy leads to a widening of the bands due to additional identification uncertainty (see figure 12 in Appendix C).

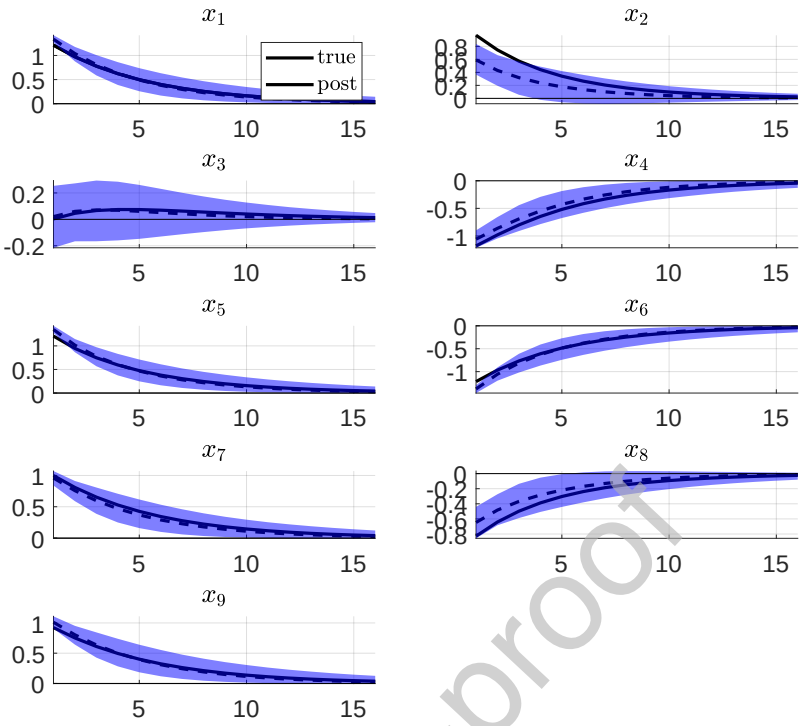

Figure 1: ***Numerical Illustration: Impulse Responses (DGP1).*** *Posterior draws of the impulse responses of informational series and corresponding true values for DGP1. The shaded area shows 80% quantiles of posterior draws pooled across simulations. The dashed line is the posterior median, while the solid line is the true impulse response.*

4 Two Applications

Having presented the model setup and the algorithm in a generic framework, this section applies the BP-FAVAR to two classical questions: (i) What are the effects of monetary policy shocks? (ii) What are the effects of shocks in the global oil market? Both questions have been addressed using small-scale Proxy VAR models (see Caldara and Herbst, 2019 and Känzig, 2019 respectively). I show how the BP-FAVAR can be employed to broaden the analysis along two dimensions. First, it allows to trace out the effect of the identified shocks on disaggregated series in a single unified model. Second, it avoids having to measure broad economic concepts such as "output", "price level", or "financial conditions" using a single, narrowly defined variable.

4.1 Monetary policy shocks

A first example for the use of Proxy VAR models is the identification of monetary policy shocks using identification based on high-frequency data. This identification scheme has been employed, among others, by Gertler and Karadi (2015) and, more recently, by Caldara and Herbst (2019). I revisit the question of how monetary policy shocks affect the economy during the Great Moderation using the proxy proposed by Caldara and Herbst (2019). I broaden their analysis using the BP-FAVAR model. This larger model setup allows to control for broad economic conditions and to trace out the effects of monetary policy shocks on various spread measures.

R	DIC
1	-445.52
2	-774.16
3	-15,731.83
4	**-20,805.97**
5	-16,949.75
6	-17,397.76
7	-12,164.10
8	-12,778.51

Table 1: ***Deviance Information Criterion (Monetary policy application).*** *Deviance Information Criterion (DIC) by Spiegelhalter et al. (2002). The preferred model minimises the DIC. The sampler is run $R_{max} = 8$ times for 20,000 draws, discarding the first 2,000 draws. See Appendix B for details.*

I estimate the BP-FAVAR using for $\boldsymbol{z_t}$ the average effective federal funds rate over the last week of the month, as Caldara and Herbst (2019). I extract latent factors from $\boldsymbol{x_t}$ which contains 128 variables from the monthly FRED dataset by McCracken and Ng (2016) (see Table 9 in Appendix D for a detailed description).[4] This model setup with a single observed factor is taken from Bernanke et al. (2005). As a proxy I use the surprises in the current federal funds future rate around Federal Open Market Committee (FOMC) meetings, as computed by Caldara and Herbst (2019). Figure 13 in Appendix D plots the proxy. The sample length is constrained by this proxy and runs from 1992M1 to 2007M6. The lag length is $P = 7$ months, following one of the specifications in Bernanke et al., 2005.

[4]Data set available at https://research.stlouisfed.org/econ/mccracken/fred-databases/

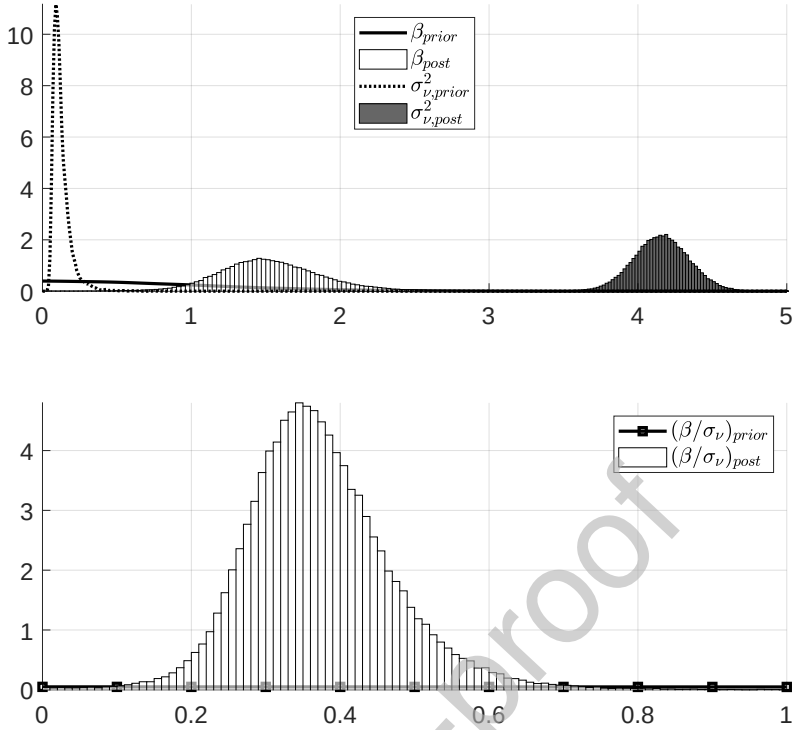

Figure 2: ***Monetary Policy Application (Caldara and Herbst, 2019): Instrument Relevance.*** *Top panel: Update of β and σ^2_ν. The prior for β is standard normal, while the prior for σ^2_ν follows an inverse Gamma distribution. Bottom panel: Update of the signal-to-noise ratio, β/σ_ν.*

The choice of the number of factors is based on the Deviance Information Criterion (DIC). To compute the DIC, the sampler is run 8 times in an initial step, varying R between 1 and 8. Table 1 shows the associated values of the DIC, which takes its minimum at 4, suggesting to set $R = 4$. Figure 14 in Appendix D shows the posterior median and 90% bands of the latent factors estimated using a Kalman filter together with the PC estimate. The posterior distribution of the latent factors differs from the PC estimate, especially for the first factor, suggesting that taking into account estimation uncertainty in the factors is important for the model dynamics.

Figure 2 shows the updating of β, σ^2_ν, and of the signal-to-noise ratio (SNR), β/σ_ν. The SNR measures how much information the instrument contains about the shock of interest compared to its noise, as pointed out by Caldara and Herbst (2019). I employ the uninformative inverse-Gamma prior for σ^2_ν and a standard-normal prior for β. Figure 2 shows that the data updates the prior belief on β and σ_ν (top panel) and that

the instrument is informative about the shock of interest given that the posterior probability mass of the SNR is away from 0 and centred around 0.4 (bottom panel). This assessment of instrument relevance could be considered a Bayesian adaptation of the weak-instrument diagnostics developed in Olea et al. (forthcoming). Given the evidence for instrument relevance there is no a priori need for conducting weak-instrument robust inference. The choice of the prior for σ_ν is important to incorporate prior information about the informativeness of the proxy. Following Caldara and Herbst (2019) I explore the implications of using their "high-relevance" prior described in the previous section. Figure 16 in Appendix D confirms that this alternative prior leads to a higher posterior SNR centred around 0.8, but leaves the main results unchanged (see Figure 17 in Appendix D).

Figure 3 shows the updating of $\boldsymbol{b}$, the impact effect of a one standard deviation monetary policy shock on the latent and observable factors. The prior distribution is not available in closed form but is implicit in the prior distributions of Σ, β and σ_ν. In order to gauge the informativeness of the instrument, I impose the prior mean for β, i.e. setting $\beta = 0$, so that all rotation vectors, $Q_{\cdot,1}$, are accepted with equal probability and the instrument is not employed for identification. A draw from the prior of $\boldsymbol{b}|\beta = 0$ is computed as follows:

- Draw Σ^{prior} from its prior inverse Wishart distribution
- Draw $Q_{\cdot,1}^{prior}$ as the first column of a draw from the uniform Haar distribution
- Compute $\boldsymbol{b}^{prior} = chol(\Sigma)Q_{\cdot,1}$.

As pointed out by Baumeister and Hamilton (2015), a uniform prior on $Q_{\cdot,1}$ does not necessarily imply a uniform distribution over the structural parameters of interest, which in this case are the elements of $\boldsymbol{b}$. The prior of $\boldsymbol{b}|\beta = 0$ implicit in the specification covers the relevant parameter space well and is updated by the data, suggesting that non-zero posterior effects are driven primarily by information from the data and the instrument. A one standard deviation monetary policy shock moves the federal funds rate by roughly 10 basis points, while the scale of the response of factors does not have a direct interpretation.

Figure 4 shows the impulse responses to a monetary policy shock normalised to generate a 25 basis points increase in the federal funds rate.[5] The median impact effect

[5]Following Caldara and Herbst (2019), posterior bands are computed based on point-wise quantiles. Extensions to joint inference such as Montiel Olea and Plagborg-Møller (2019) and Inoue and Kilian (2020) are generally feasible.

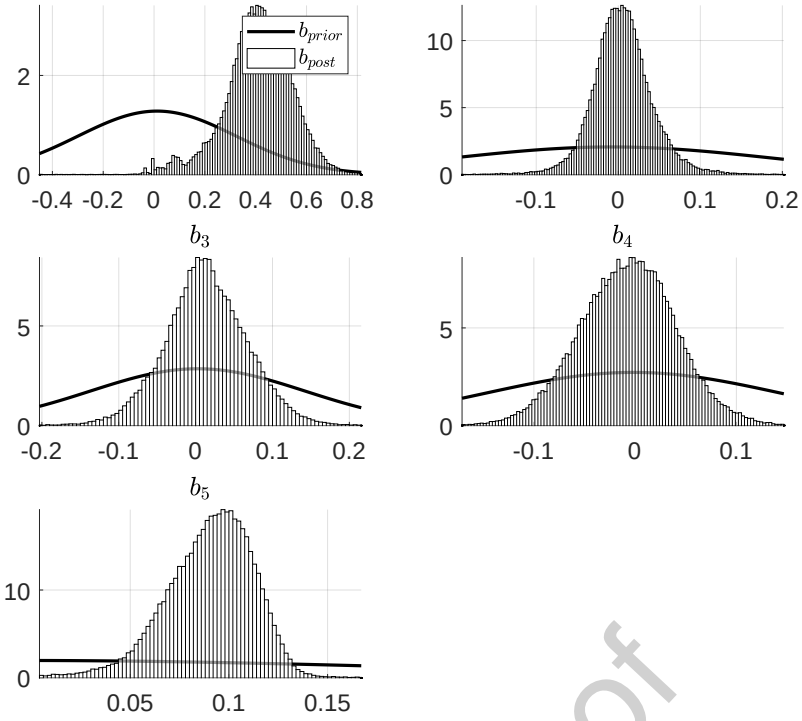

Figure 3: ***Monetary Policy Application (Caldara and Herbst, 2019): Updating of b.*** *Priors (solid line) and posterior (histogram) of* $\mathbf{b}$*. Prior draws are computed from the distribution implicit in the priors for* Σ*,* β *and* σ_ν*.*

on government bond spreads over the federal funds rate is stronger in the medium run the longer the maturity of the underlying treasury bill. In the medium run, the drop in spreads of longer maturity, as well as that of corporate bonds, is more pronounced and reaches up to -40 basis points. This drop in the term premium of long term bonds is consistent with the findings in Rudebusch and Swanson (2012) and Crump et al. (2017) and explained by investor's increased willingness to invest in longer-term bonds following a monetary tightening.

Miranda-Agrippino and Ricco (2018) argue that market-based proxies for monetary policy shocks such as the ones in Gertler and Karadi (2015) and Caldara and Herbst (2019) combine an exogenous policy shock with additional information about the state of the economy revealed by the central bank through their statement. Miranda-Agrippino and Ricco (2018) propose a proxy that addresses this rigid information issue by projecting market-based monetary surprises on their own lags, and on Greenbook forecasts. When employing this proxy, I find that it has a lower posterior SNR centred around 0.2 (see figure 20 in Appendix D), suggesting that this proxy is weaker than the one by Caldara and Herbst (2019). Figure 22 in Appendix D shows the impulse responses when employing this proxy. While the estimated impact effects are slightly changed, the medium-term drop in the 5-year, the 10-year and the corporate bond spreads, remains

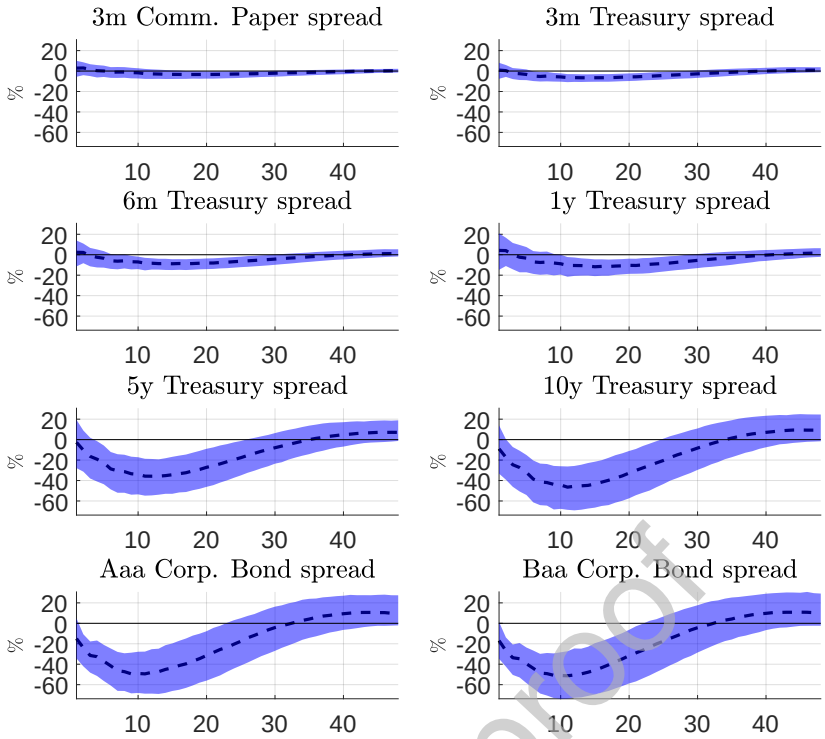

Figure 4: ***Monetary Policy Application (Caldara and Herbst, 2019): Impulse Response Functions of informational series.*** *Point-wise median impulse responses (solid line) with 68% bands. The model includes $R = 4$ latent factors. The impact effect is normalised to generate a 0.25% increase in the observable factor. The spread is computed with respect to the federal funds rate (see table 9 in Appendix D). The proxy by Caldara and Herbst (2019) is used for identification.*

and is quantitatively similar, suggesting robustness of the results with respect to the choice of proxy.

4.2 Oil market shocks

The second example for the use of Proxy VAR models is a study of the effects of global oil prices on the US economy. Estimating this causal effect is difficult given the two-way feedback between oil prices and the US economy. That is why several studies introduce narrative information about the global oil market in order to achieve identification. Examples are Kilian (2008), Caldara et al. (2019), and, more recently, Känzig (2019).

I revisit the issue of the effects of oil supply news shocks on the US economy using the proxy proposed by Känzig (2019). I augment the baseline model by latent factors extracted from US series and trace out the effects of oil supply news on various US

series in a unified model. In addition, I reproduce the result that exogenous negative news about future oil supply leads to a drop in oil prices and a a fall in world economic activity.

The data contained in $\boldsymbol{z}_t$ are four series commonly used for modelling the global oil market (see Kilian, 2009, Baumeister and Hamilton, 2019, Känzig, 2019): World oil production, world industrial production, the WTI oil spot price, and world oil inventories. All variables enter in log levels, as in Känzig (2019). I use a lag length of $P = 13$, following Känzig (2019). The vector of observational series, $\boldsymbol{x}_t$, contains 128 monthly series from the FRED dataset by McCracken and Ng (2016) (see Appendix D for a detailed description).

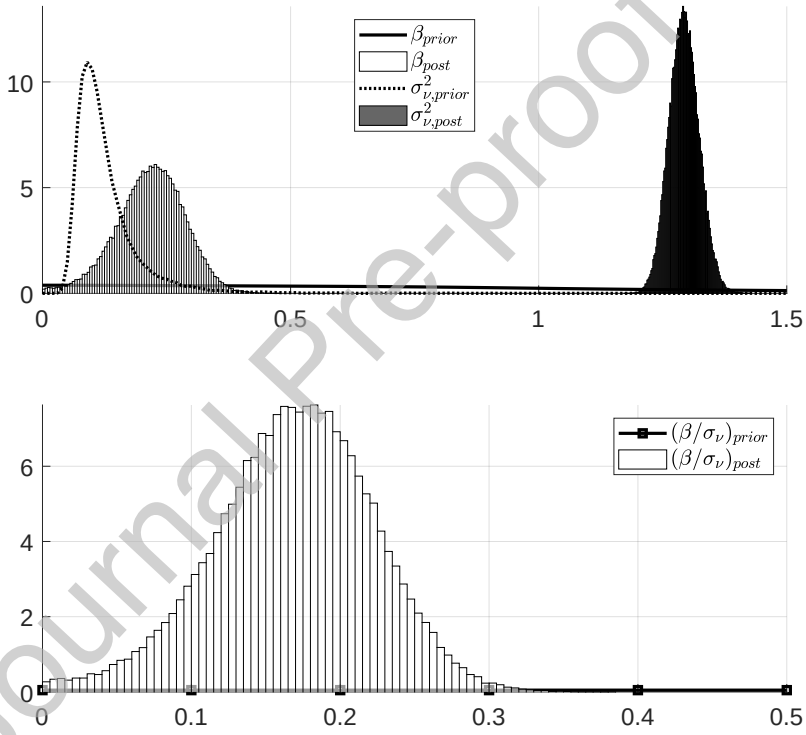

Figure 5: ***Oil market application: Instrument Relevance.*** *Top panel: Update of β and σ^2_ν. The prior for β is standard normal, while the prior for σ^2_ν follows an inverse Gamma distribution. Bottom panel: Update of the signal-to-noise ratio, β/σ_ν.*

As an instrument I employ the Känzig (2019) narrative measure of oil supply news shocks. It is motivated by the oil market having one big player, the Organization of the Petroleum Exporting Countries (OPEC) which accounts for 44 percent of the world's

crude oil production. The OPEC makes regular announcements about its production plans. These announcements influence the highly liquid futures market for crude oil, allowing to apply the Gertler and Karadi (2015) high-frequency identification strategy to the oil market: Surprise oil market news shocks are measured as jumps in West Texas Intermediate (WTI) crude oil market futures in tight windows around OPEC announcements. Assuming that global economic conditions are priced into WTI crude oil futures before the announcement and assuming that OPEC announcements are the only drivers of prices within this window, this measure arguably captures changes in oil price expectations caused by OPEC announcements. Therefore it can be considered exogenous to the global oil market. Figure 23 in Appendix D plots the instrument.[6]

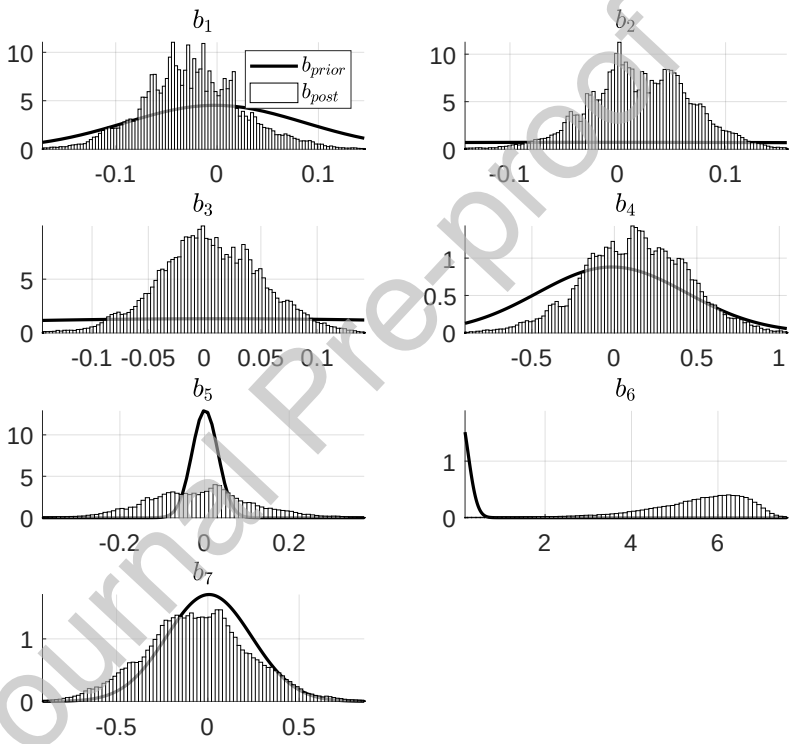

Figure 6: ***Oil market Application: Updating of b.*** *Priors (solid line) and posterior (histogram) of* $\mathbf{b}$*. Prior draws are computed from the distribution implicit in the priors for* Σ*,* β *and* σ_ν*.*

I augment the baseline model by $R = 3$ latent factors, based on the DIC (see Table 7 in Appendix A.1). Figure 24 in Appendix D shows the latent factors estimated via the

[6]The proxy is non-zero for the majority of time-periods, lending support to the use of a normal distribution in equation 7 as an approximation.

Carter-Kohn procedure employed in the BP-FAVAR model together with a Principal Components estimate. The Principal Components estimate fails to take into account the estimation uncertainty in the latent factors, treating them as observed data in the transition equation. Thereby using Principal Components yields a skewed view of the overall estimation uncertainty.

Figure 5 shows the updating of β and σ_ν^2. There is evidence that the uninformative priors for both are updated by the data (top panel) with a posterior of β centred around 0.3 and a posterior of σ_ν^2 centred around 1.3. This finding translates into a posterior SNR centred around 0.18 (bottom panel), suggesting that the proxy by Känzig (2019) is informative about oil supply news shocks. Employing a high-relevance prior increases the posterior mean of the SNR to 0.4, but leaves the main results unchanged (see Figures 26 and 27 in Appendix D).

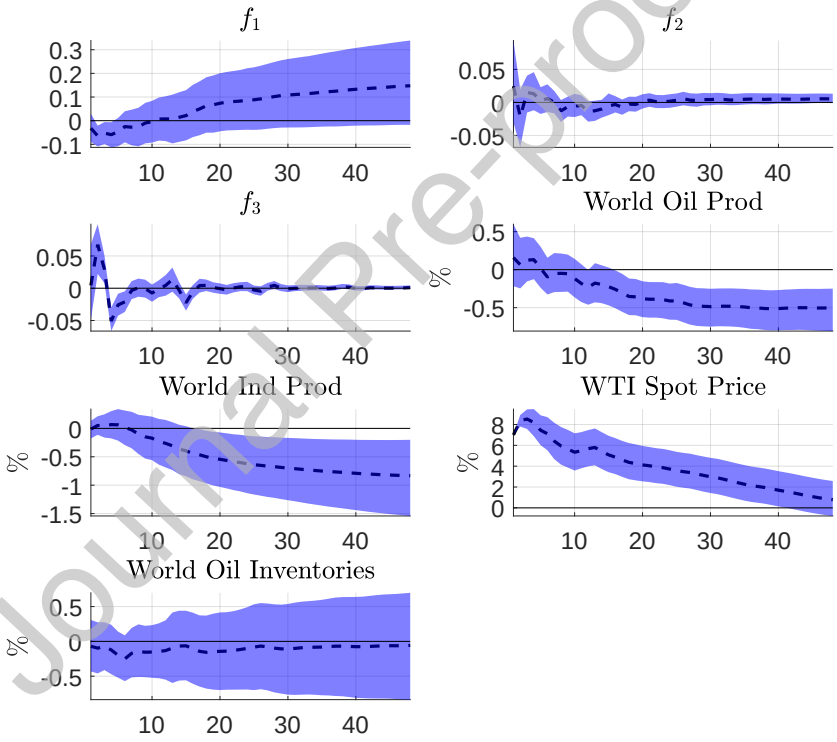

Figure 7: ***Impulse Response Functions of observable variables and latent factors (Oil market application).*** *Point-wise median impulse responses (solid line) with 68% bands. The model includes $R = 3$ latent factors. The impact effect is normalised to generate a 7% increase in the WTI spot price. The proxy by Känzig (2019) is used for identification*

Figure 6 shows the update of the impact effect of a one standard deviation oil supply news shocks on latent and observable factors. The implicit prior on $\boldsymbol{b}$, calculated as in the previous section, is clearly updated by the data, suggesting that a one standard deviation shock increases the WTI spot price (b_7) by roughly 6 per cent, while the impact effects of the remaining factors are centred around 0.

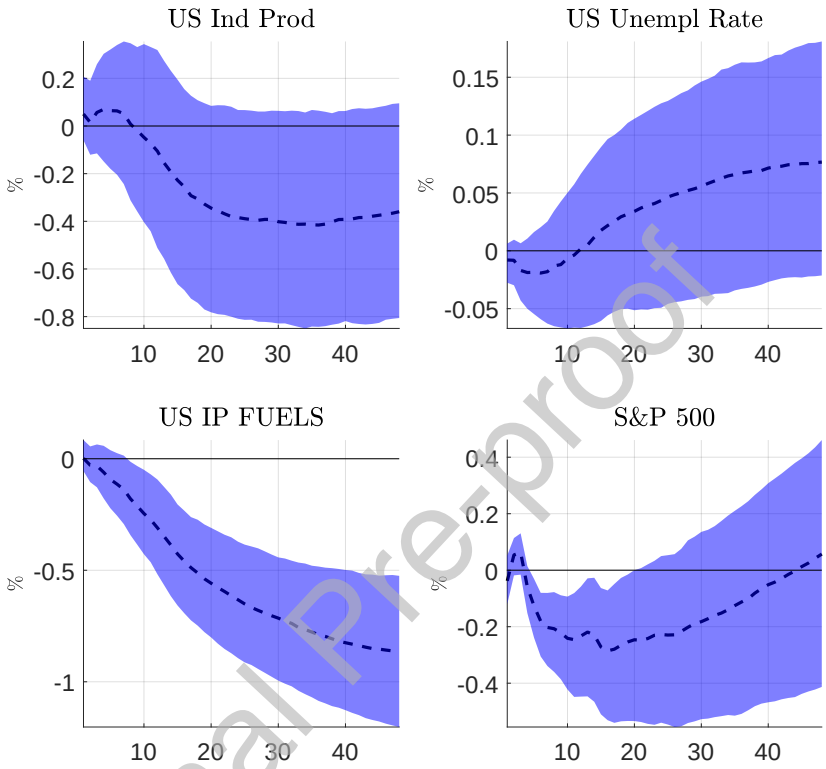

Figure 8: ***Impulse Response Functions of informational series (Oil market application).*** *Point-wise median impulse responses (solid line) with 68% bands. The model includes $R = 3$ latent factors. The impact effect is normalised to generate a 7% increase in the WTI spot price. The proxy by Känzig (2019) is used for identification.*

Figure 7 shows the posterior impulse responses of latent and observable factors to an oil supply news shock normalised to generate a 7 per cent increase in the WTI spot price.[7] There is evidence that an oil supply news shock, which increases oil prices, leads to a decrease in median world oil production and a decrease in median world industrial production after 18 months of 0.3% and 0.8 %, respectively. These results qualitatively confirm the findings in Känzig (2019). The effect on oil inventories is not distinguishable

[7]This normalisation is chosen for camparability with Känzig (2019).

from 0.

Figure 8 shows the associated impulse responses of selected informational series. US industrial production decreases up to 0.4%, while the subcomponent related to fuel production decreases more strongly, up to 0.8% following an oil supply news shock. US unemployment tends to increase up to 0.1%. The S&P 500 stock market index drops by 0.2% in the medium run and then rebounds within 4 years. These results confirm the adverse effects of negative news about future oil supply on the US real economy and US stock markets found in Känzig (2019).

5 Conclusion

This paper proposes a Bayesian approach to investigate the dynamic causal effects of structural shocks identified via proxies in a data-rich environment. Adding latent factors to standard small-scale VAR models has two advantages: It allows controlling for broad economic concepts, avoiding measuring these concepts using narrowly defined variables. Second, the reaction of disaggregated series can be traced out within a single, unified model.

In a first application to monetary policy I find that monetary policy shocks identified using high-frequency proxies yield effects which differ across the yield curve. In a second application to global oil market shocks I find that negative news about future oil supply, identified via OPEC announcements, have sizeable adverse effects on the US economy.

References

Amir-Ahmadi, P. and Uhlig, H. (2015), 'Sign restrictions in Bayesian FAVARs with an application to monetary policy shocks', *NBER Working paper 21738* .

Arias, J. E., Rubio-Ramirez, J. F. and Waggoner, D. (2018), Inference in Bayesian proxy-svars, Technical report, Federal Reserve Bank of Atlanta.

Bahaj, S. (2020), 'Sovereign spreads in the euro area: Cross border transmission and macroeconomic implications', *Journal of Monetary Economics* **110**, 116–135.

Baumeister, C. and Hamilton, J. D. (2015), 'Sign restrictions, structural vector autoregressions, and useful prior information', *Econometrica* **83**(5), 1963–1999.

Baumeister, C. J. and Hamilton, J. D. (2019), 'Structural interpretation of vector autoregressions with incomplete identification: Revisiting the role of oil supply and demand shocks', *The American Economic Review* **109**(5), 1873–1910.

Belviso, F. and Milani, F. (2006), 'Structural factor-augmented VARs (SFAVARs) and the effects of monetary policy', *Topics in Macroeconomics* **6**(3).

Bernanke, B. S., Boivin, J. and Eliasz, P. (2004), Measuring the effects of monetary policy: A factor-augmented vector autoregressive (FAVAR) approach, Technical report, National Bureau of Economic Research.

Bernanke, B. S., Boivin, J. and Eliasz, P. (2005), 'Measuring the effects of monetary policy: a factor-augmented vector autoregressive (FAVAR) approach', *The Quarterly Journal of Economics* **120**(1), 387–422.

Caldara, D., Cavallo, M. and Iacoviello, M. (2019), 'Oil price elasticities and oil price fluctuations', *Journal of Monetary Economics* **103**, 1–20.

Caldara, D. and Herbst, E. (2019), 'Monetary policy, real activity, and credit spreads: Evidence from Bayesian proxy SVARs', *American Economic Journal: Macroeconomics* **11**(1), 157–92.

Carter, C. K. and Kohn, R. (1994), 'On Gibbs sampling for state space models', *Biometrika* **81**(3), 541–553.

Chan, J. C. and Eisenstat, E. (2018), 'Bayesian model comparison for time-varying parameter vars with stochastic volatility', *Journal of applied econometrics* **33**(4), 509–532.

Chan, J. C. and Grant, A. L. (2016), 'On the observed-data deviance information criterion for volatility modeling', *Journal of Financial Econometrics* **14**(4), 772–802.

Cowles, M. K. and Carlin, B. P. (1996), 'Markov Chain Monte Carlo convergence diagnostics: a comparative review', *Journal of the American Statistical Association* **91**(434), 883–904.

Crump, R. K., Eusepi, S., Moench, E. et al. (2017), 'The term structure of expectations and bond yields', *Federal Reserve Bank of New York Staff Reports, No.775* .

Del Negro, M. and Schorfheide, F. (2011), 'Bayesian Macroeconometrics', *Handbook of Macroeconomics* pp. 293–389.

Drautzburg, T. (2016), A narrative approach to a fiscal DSGE model, Technical report, Federal Reserve Bank of Philadelphia.

Frühwirth-Schnatter, S. (1994), 'Data augmentation and dynamic linear models', *Journal of time series analysis* **15**(2), 183–202.

Gertler, M. and Karadi, P. (2015), 'Monetary policy surprises, credit costs, and economic activity', *American Economic Journal: Macroeconomics* **7**(1), 44–76.

Geweke, J. (1992), 'Evaluating the accuracy of sampling-based approaches to the calculation of posterior moments', *Bayesian Statistics* **4**, 169–193.

Huber, F. and Fischer, M. M. (2018), 'A Markov switching factor-augmented VAR model for analyzing US business cycles and monetary policy', *Oxford Bulletin of Economics and Statistics* **80**(3), 575–604.

Inoue, A. and Kilian, L. (2020), 'Joint bayesian inference about impulse responses in VAR Models', *manuscript, Federal Reserve Bank of Dallas* .

Känzig, D. R. (2019), 'The macroeconomic effects of oil supply shocks: New evidence from OPEC announcements', *Available at SSRN 3185839* .

Kerssenfischer, M. (2019), 'The puzzling effects of monetary policy in VARs: Invalid identification or missing information?', *Journal of Applied Econometrics* **34**(1), 18–25.

Kilian, L. (2008), 'Exogenous oil supply shocks: how big are they and how much do they matter for the US economy?', *The Review of Economics and Statistics* **90**(2), 216–240.

Kilian, L. (2009), 'Not all oil price shocks are alike: Disentangling demand and supply shocks in the crude oil market', *American Economic Review* **99**(3), 1053–69.

Kilian, L. and Lütkepohl, H. (2017), *Structural vector autoregressive analysis*, Cambridge University Press.

Kose, M. A., Otrok, C. and Whiteman, C. H. (2003), 'International business cycles: World, region, and country-specific factors', *american economic review* **93**(4), 1216–1239.

Lopes, H. F. and West, M. (2004), 'Bayesian model assessment in factor analysis', *Statistica Sinica* pp. 41–67.

McCracken, M. W. and Ng, S. (2016), 'Fred-md: A monthly database for macroeconomic research', *Journal of Business & Economic Statistics* **34**(4), 574–589.

Miescu, M. S. and Mumtaz, H. (2019), Proxy structural vector autoregressions, informational sufficiency and the role of monetary policy, Technical report, Queen Mary University of London, School of Economics and Finance.

Miranda-Agrippino, S. and Ricco, G. (2018), The transmission of monetary policy shocks, Technical report, CEPR Discussion Papers.

Montiel Olea, J. L. and Plagborg-Møller, M. (2019), 'Simultaneous confidence bands: Theory, implementation, and an application to SVARs', *Journal of Applied Econometrics* **34**(1), 1–17.

Mumtaz, H. and Surico, P. (2012), 'Evolving international inflation dynamics: world and country-specific factors', *Journal of the European Economic Association* **10**(4), 716–734.

Mumtaz, H. and Theophilopoulou, A. (2019), Monetary policy and wealth inequality over the great recession in the uk an empirical analysis, Technical report, Queen Mary University of London, School of Economics and Finance.

Olea, J. L. M., Stock, J. H. and Watson, M. W. (forthcoming), 'Inference in structural VARs with External Instruments', *Journal of Econometrics* .

Primiceri, G. E. (2005), 'Time varying structural vector autoregressions and monetary policy', *The Review of Economic Studies* **72**(3), 821–852.

Raftery, A. and Lewis, S. (1992), 'How many iterations in the Gibbs sampler?', *Bayesian Statistics* **4**, 763–773.

Rubio-Ramirez, J. F., Waggoner, D. F. and Zha, T. (2010), 'Structural vector autoregressions: Theory of identification and algorithms for inference', *The Review of Economic Studies* **77**(2), 665–696.

Rudebusch, G. D. and Swanson, E. T. (2012), 'The bond premium in a dsge model with long-run real and nominal risks', *American Economic Journal: Macroeconomics* **4**(1), 105–43.

Spiegelhalter, D. J., Best, N. G., Carlin, B. P. and Van Der Linde, A. (2002), 'Bayesian measures of model complexity and fit', *Journal of the royal statistical society: Series b (statistical methodology)* **64**(4), 583–639.

Stock, J. H. and Watson, M. W. (2012), 'Disentangling the channels of the 2007-2009 recession', *NBER Working paper 18094* .

Stock, J. H. and Watson, M. W. (2016), 'Dynamic factor models, factor-augmented vector autoregressions, and structural vector autoregressions in macroeconomics', *Handbook of macroeconomics* **2**, 415–525.

Stock, J. H. and Watson, M. W. (2018), 'Identification and estimation of dynamic causal effects in macroeconomics using external instruments', *The Economic Journal* **128**(610), 917–948.

Yamamoto, Y. (2019), 'Bootstrap inference for impulse response functions in factor-augmented vector autoregressions', *Journal of Applied Econometrics* **34**(2), 247–267.

Yu, J. and Meyer, R. (2006), 'Multivariate stochastic volatility models: Bayesian estimation and model comparison', *Econometric Reviews* **25**(2-3), 361–384.

A Posterior Inference

A.1 Conditional posterior of F

The procedure to generate posterior draws of latent factors, F, differs from generating draws of parameters, in that one has to generate the whole dynamic evolution of factors for each $t = 1, ..., T$. For this to be feasible I exploit the Markov property of the system described in equation (3) as follows:

$$p(\begin{bmatrix} Y \\ m \end{bmatrix} | X, \theta) = p(\begin{bmatrix} \boldsymbol{y}_t \\ m_t \end{bmatrix} | X, \theta) \prod_{t=1}^{T-1} p(\begin{bmatrix} \boldsymbol{y}_t \\ m_t \end{bmatrix} | \begin{bmatrix} \boldsymbol{y}_{t+1} \\ m_{t+1} \end{bmatrix}, X, \theta). \tag{22}$$

First note that (22) describes the posterior of $\begin{bmatrix} Y \\ m \end{bmatrix}$, which contains both latent and observable factors and the proxy. The reason for including the observable factors and the proxy is the dynamic interdependence between latent and observable factors and the proxy, which needs to be accounted for. Given that the observable factors and the proxy are non-random, their distribution has a zero variance.[8] Second, note that this is a product of $(R + K + 1)$-dimensional conditional distributions. Given the assumption of Gaussianity of $\boldsymbol{\xi}_t$ and $\boldsymbol{u}_t$, this representation can be combined with the observation equation (1) and is amenable to the Carter-Kohn algorithm described in Carter and Kohn (1994) and Frühwirth-Schnatter (1994).

A.1.1 State-space form

Start by rewriting observation equation (1) and transition equation (3) as

$$\begin{bmatrix} \boldsymbol{x}_t \\ \boldsymbol{z}_t \\ m_t \end{bmatrix} = \mathcal{H}\mathcal{B}_t + \mathcal{W}_t \tag{23}$$

$$\mathcal{B}_t = \mathcal{F}\mathcal{B}_{t-1} + \mathcal{V}_t \tag{24}$$

$$Var(\mathcal{W}_t) = \mathcal{R} \tag{25}$$

$$Var(\mathcal{V}_t) = \mathcal{Q} \tag{26}$$

[8] Here, I refer to the variance across draws. The variance across time is, of course, non-zero.

where

$$\mathcal{H} = \begin{bmatrix} \Lambda^f & \Lambda^z & 0 & ... & 0 \\ \mathbf{0} & I & 0 & ... & 0 \\ \mathbf{0} & \mathbf{0} & 1 & ... & 0 \end{bmatrix}; \quad \mathcal{B}_t = \begin{bmatrix} \lfloor_t' & \lfloor_{t-1}' & ... & \lfloor_{t-p}' \end{bmatrix}'; \quad \lfloor_t = \begin{bmatrix} \boldsymbol{f}_t \\ \boldsymbol{z}_t \\ m_t \end{bmatrix}$$

$$\mathcal{W}_t = \begin{bmatrix} \boldsymbol{\xi}_t \\ \mathbf{0} \\ 0 \end{bmatrix}; \quad \mathcal{F} = \begin{bmatrix} \Pi_1 & 0 & \Pi_2 & 0 & ... & \Pi_p & 0 \\ & & & \mathbf{0} & & & \\ & & & I & \mathbf{0} & & \end{bmatrix}; \quad \mathcal{V}_t = \begin{bmatrix} \boldsymbol{u}_t \\ m_t \\ \mathbf{0} \end{bmatrix}$$

$$\mathcal{R} = \begin{bmatrix} \Omega & \mathbf{0} \\ \mathbf{0} & \mathbf{0} \end{bmatrix}; \quad \mathcal{Q} = \begin{bmatrix} \Sigma & chol(\Sigma)Q\boldsymbol{\beta} & \mathbf{0} \\ \boldsymbol{\beta}'Q'chol(\Sigma)' & \boldsymbol{\beta}'\boldsymbol{\beta} + \sigma_\nu^2 & \mathbf{0} \\ \mathbf{0} & \mathbf{0} & \mathbf{0} \end{bmatrix},$$

where $\boldsymbol{\beta} = [\beta \quad \mathbf{0}]'$.

Then consider the following factorisation:

$$p(\mathcal{B}_{1:T}|X, \boldsymbol{\theta}) = p(\mathcal{B}_T|\boldsymbol{x}_{1:T}, \boldsymbol{\theta}) \prod_{t=1}^{T-1} p(\mathcal{B}_t|\mathcal{B}_{t+1}, X, \theta) \tag{27}$$

Given the linear Gaussian form of the state space model we have that

$$\mathcal{B}_T|\boldsymbol{x}_{1:T}, \theta \sim N(\mathcal{B}_{T|T}, \mathcal{P}_{T|T}) \tag{28}$$

$$\mathcal{B}_{t|T}|\mathcal{B}_{t+1|T}, \boldsymbol{x}_{1:T}, \theta \sim N(\mathcal{B}_{t|t,\mathcal{B}_{t+1|T}}, \mathcal{P}_{t|t,\mathcal{B}_{t+1|T}}) \tag{29}$$

with

$$\mathcal{B}_{T|T} = E(\mathcal{B}_T|\boldsymbol{x}_{1:T}, \boldsymbol{\theta}) \tag{30}$$

$$\mathcal{P}_{T|T} = Cov(\mathcal{B}_T|\boldsymbol{x}_{1:T}, \boldsymbol{\theta}) \tag{31}$$

$$\mathcal{B}_{t|t,\mathcal{B}_{t+1|T}} = E(\mathcal{B}_t|\mathcal{B}_{t|t}, \mathcal{B}_{t+1|t}, \boldsymbol{\theta}) \tag{32}$$

$$\mathcal{P}_{t|t,\mathcal{B}_{t+1|T}} = Cov(\mathcal{B}_t|\mathcal{B}_{t|t}, \mathcal{B}_{t+1|t}, \boldsymbol{\theta}) \tag{33}$$

A.1.2 Carter-Kohn algorithm

In a first step, we can run a Kalman filter to obtain a series of Kalman-filtered draws of the state variable $\mathcal{B}_t$ $\mathcal{B}_{t|t}$ for $t = 1, ...T$. To initialise, we set $\mathcal{B}_{1|0} = 0$ and $\mathcal{P}_{1|0} = \mathbf{I}$.

Then, iterate forward as:

$$\mathcal{B}_{t|t} = \mathcal{B}_{t|t-1} + \kappa_{t|t-1}\eta_{t|t-1} \tag{34}$$

where $\eta_{t|t-1} = \mathcal{B}_t - \mathcal{F}\mathcal{B}_{t|t-1}$ denotes the forecast error, $\mathfrak{f}_{t|t-1} = \mathcal{H}\mathcal{P}_{t|t-1}\mathcal{H}' + \mathcal{R}$ its variance and $\kappa_{t|t-1} = \mathcal{P}_{t|t-1}\mathcal{H}\mathfrak{f}_{t|t-1}^{-1}$ the "Kalman-gain"

$$\mathcal{P}_{t|t-1} = \mathcal{F}\mathcal{P}_{t-1|t-1}\mathcal{F}' + \mathcal{Q} \tag{35}$$

Then, conditioning on the last of these Kalman-filtered draws, $\mathcal{B}_{T|T}$ and $\mathcal{P}_{T|T}$, we can run the filter backwards to obtain a series $\mathcal{B}_{t|t+1}$ for $t = 1, ..., T-1$ as follows:

$$\mathcal{B}^*_{t|t,\mathcal{B}_{t+1|T}} = \mathcal{B}_{t|t} + \mathcal{P}_{t|t}\mathcal{F}^{*'}J^{-1}_{t+1|t}\psi_{t+1|t} \tag{36}$$

$$\mathcal{P}^*_{t|t,\mathcal{B}_{t+1|T}} = \mathcal{P}_{t|t} - \mathcal{P}_{t|t}\mathcal{F}^{*'}J^{-1}_{t+1|t}\mathcal{F}^*\mathcal{P}_{t|t} \tag{37}$$

where $\psi_{t+1|t} = \mathcal{B}^*_{t+1} - \mathcal{F}^*\mathcal{B}_{t|t}$ and $J_{t+1|t} = \mathcal{F}^*P_{t|t}\mathcal{F}^{*'} + \mathcal{Q}^*$. Note that $\mathcal{Q}^*$ refers to the top $R \times R$ block of $\mathcal{Q}$ and that $\mathcal{F}^*$ and $\mathcal{B}^*$ denote the first R rows of $\mathcal{F}$ and $\mathcal{B}$, respectively. This is required because $\mathcal{Q}$ is singular given the presence of observable factors.

Plugging these draws into (27) results in an unconditional posterior draw of the state variable, $\mathcal{B}_1, ..., \mathcal{B}_T$. Its top $R + K$ block represents an unconditional posterior draw of factors, $\boldsymbol{y}_t$.

A.2 Conditional posterior of $\{\Lambda, \Omega\}$

This section discusses conditional posterior inference on $\{\Lambda, \Omega\}$. It draws partially on Bernanke et al. (2004). Restate the observation equation for convenience

$$\boldsymbol{x}_t = \Lambda^f \boldsymbol{f}_t + \Lambda^z \boldsymbol{z}_t + \boldsymbol{\xi}_t \tag{38}$$

$$\boldsymbol{\xi}_t \sim N(\boldsymbol{0}, \Omega) \tag{39}$$

with $\Lambda = [\lambda^f \quad \lambda^z]$. Given a draw of the latent and observable factors, $\boldsymbol{y}_t = [\boldsymbol{f}_t' \quad \boldsymbol{z}_t']'$, and under the assumption that Ω is diagonal, (38) amounts to N independent linear regressions.

Assuming (conjugate) normal-inverse Gamma priors of the form

$$\boldsymbol{\omega}_{ii} \sim IG(sc^*, sh^*) \tag{40}$$

$$\boldsymbol{\lambda}_i|\boldsymbol{\omega}_{ii} \sim N(\boldsymbol{\mu}^*_{\lambda,i}, \boldsymbol{\omega}_{ii} M_i^{*-1}), \tag{41}$$

delivers posterior distributions of the form

$$\boldsymbol{\omega}_{ii} \sim IG(sc, sh) \tag{42}$$

$$\boldsymbol{\lambda}_i|\boldsymbol{\omega}_{ii} \sim N(\boldsymbol{\mu}_{\lambda,i}, \boldsymbol{\omega}_{ii} M_i^{-1}), \tag{43}$$

with

$$\begin{aligned}
sh &= sc^* + T \\
sc &= sc^* + \hat{\xi}_i \hat{\xi}_i{}' + (\hat{\lambda}_i - \boldsymbol{\mu}^*_{\lambda,i})'(M_i^{*-1} + (Y_i Y_i')^{-1})(\hat{\lambda}_i - \boldsymbol{\mu}^*_{\lambda,i}) \\
M_i &= M_i^* + Y_i Y_i' \\
\boldsymbol{\mu}_{\lambda,i} &= M_i^{-1}(M_i^* \boldsymbol{\mu}^*_{\lambda,i} + Y_i Y_i')\hat{\lambda}_i,
\end{aligned}$$

where $\hat{\xi}_i$ are the fitted errors from the i-th regression and $\hat{\lambda}_i$ is the OLS estimate of λ_i, and Y_i are the regressors of the i-th equation. Note that employing uninformative priors centred around zero, i.e. setting $sc^* = 0$, $sh^* = 0$, $\boldsymbol{\mu}^*_{\lambda,i} = \mathbf{0}$, and $M_i^{*-1} = 0$ collapses the posterior towards the OLS estimate:

$$\begin{aligned}
sh &= T \\
sc &= \hat{\xi}_i \hat{\xi}_i{}' \\
M_i &= Y_i Y_i' \\
\boldsymbol{\mu}_{\lambda,i} &= \hat{\lambda}_i,
\end{aligned}$$

A.3 Conditional posterior of $\{\Sigma, \Pi\}$

This section discusses conditional posterior inference on $\{\Sigma, \Pi\}$. It proceeds in two steps: First, generate candidate draws $\{\Pi^{cand}, \Sigma^{cand}\}$ from

$$p(\Pi, \Sigma|\Lambda^f, \Lambda^z, \Omega, F, \beta, \sigma_\nu, X, Z)$$

(note that $\boldsymbol{m}$ is not part of the conditioning set). Second, map these candidate draws into draws from the conditional target distribution,

$$p(\Pi, \Sigma | \Lambda^f, \Lambda^z, \Omega, F, \beta, \sigma_\nu, \boldsymbol{b}, X, Z, \boldsymbol{m})$$

(note that $\boldsymbol{m}$ is now part of the conditioning set).

For the first step, the derivations can be found, for example, in Kilian and Lütkepohl (2017). Restate the transition equation for convenience

$$\boldsymbol{y}_t = \Pi \boldsymbol{w}_t + \boldsymbol{u}_t \tag{44}$$

$$\boldsymbol{u}_t \sim N(\boldsymbol{0}, \Sigma), \tag{45}$$

Given a draw of latent and observable factors, $\boldsymbol{y}_t$, equation (44) is a standard VAR(P) model. Therefore, employing independent normal-inverse Wishart priors of the form

$$vec(\Pi) \sim N(\boldsymbol{\mu}_\Pi^*, V_\Pi^*) \tag{46}$$

$$\Sigma \sim IW(S^*, \tau^*), \tag{47}$$

delivers posterior distributions of the form

$$vec(\Pi)|\Sigma \sim N(\boldsymbol{\mu}_\Pi, V_\Pi) \tag{48}$$

$$\Sigma|\Pi \sim IW(S, \tau), \tag{49}$$

where

$$V_\Pi = (V_\Pi^{*-1} + (WW' \otimes \Sigma^{-1}))^{-1} \tag{50}$$

$$\boldsymbol{\mu}_\Pi = V_\Pi (V_\Pi^{*-1} + (W \otimes \Sigma^{-1}) vec(Y)) \tag{51}$$

$$S = S^* + (Y - \Pi W)(Y - \Pi W)' \tag{52}$$

$$\tau = \tau^* + T \tag{53}$$

I follow Caldara and Herbst (2019) in setting the hyperparemters of the Minnesota prior as in Del Negro and Schorfheide (2011) as $\lambda = [0.5; 3; 1; 0.5; 0.5; 1]$. Unlike their case, I implement an independent prior in order to facilitate incorporation into the Gibbs sampler. This setup is not amenable to implementation via dummy observations as in Caldara and Herbst (2019).

In a second step, $\{\Pi^{cand}, \Sigma^{cand}\}$ are mapped into draws from the conditional target distribution via a Metropolis-Hastings step. At iteration j of the sampler, this involves setting

$$\{\Pi^j, \Sigma^j\} = \begin{cases} \{\Pi^{cand}, \Sigma^{cand}\} & \text{with probability } \alpha \\ \{\Pi^{j-1}, \Sigma^{j-1}\} & \text{with probability } (1-\alpha) \end{cases}, \tag{54}$$

where

$$\alpha = min(\frac{p(\Pi_{cand}, \Sigma_{cand}|\Lambda^{f,j}, \Lambda^{z,j}, \Omega^j, F^j, \beta^j, \sigma_\nu^j, \boldsymbol{b}^j, X, Z, \boldsymbol{m})}{p(\Pi^{j-1}, \Sigma^{j-1}|\Lambda^{f,j}, \Lambda^{z,j}, \Omega^j, F^j, \beta^j, \sigma_\nu^j, \boldsymbol{b}^j, X, Z, \boldsymbol{m})}, 1) \tag{55}$$

A.4 Conditional posterior of b

This section re-parametrises Caldara and Herbst (2019) to allow for identification of impact effects. For the posterior sampler, we will need to be able to evaluate the conditional likelihood of m_t given $\boldsymbol{y}_t$.

Write transition and proxy equation in stacked form for convenience and compute the unconditional variance:

$$\begin{bmatrix} \boldsymbol{y}_t \\ m_t \end{bmatrix} = \begin{bmatrix} \Pi & 0 \\ \boldsymbol{0} & 0 \end{bmatrix} \begin{bmatrix} \boldsymbol{w}_t \\ m_{t-1} \end{bmatrix} + \begin{bmatrix} B & \boldsymbol{\beta} \\ \boldsymbol{\beta}' & \sigma_\nu \end{bmatrix} \begin{bmatrix} \boldsymbol{\epsilon}_t \\ \nu_t \end{bmatrix} \tag{56}$$

$$Var(\begin{bmatrix} \boldsymbol{y}_t - \Pi \boldsymbol{w}_t \\ m_t \end{bmatrix}) = \begin{bmatrix} \boldsymbol{\Sigma} & B\boldsymbol{\beta} \\ \boldsymbol{\beta}' B' & \boldsymbol{\beta}'\boldsymbol{\beta} + \sigma_\nu^2 \end{bmatrix}, \tag{57}$$

where $\boldsymbol{\beta} = [\beta \quad \boldsymbol{0}]'$

The likelihood is invariant to observationally equivalent rotations of B. Therefore we can replace $B = B^c Q$, where B^c is, for example, the lower-triangular Cholesky decomposition of Σ.

$$Var(\begin{bmatrix} \boldsymbol{y}_t - \Pi \boldsymbol{w}_t \\ m_t \end{bmatrix}) = \begin{bmatrix} \Sigma & B^c Q \boldsymbol{\beta}' \\ \boldsymbol{\beta} Q' B^{c'} & \boldsymbol{\beta}'\boldsymbol{\beta} + \sigma_\nu^2 \end{bmatrix} \tag{58}$$

Then, using the rules for the conditional mean of multivariate normal distributions, we

obtain the conditional likelihood

$$m_t|\boldsymbol{y}_t, \Pi, \Sigma, \boldsymbol{b}, \beta, \sigma_\nu \sim N(\mu_{m|Y}, V_{m|Y}), \tag{59}$$
$$\mu_{m|Y} = \boldsymbol{\beta} Q' B^{c'} \Sigma^{-1} \boldsymbol{u}_t \tag{60}$$
$$= \beta \boldsymbol{\epsilon}_{1,t} \tag{61}$$
$$V_{m|Y} = \boldsymbol{b}\boldsymbol{b}' + \sigma_\nu^2 - \boldsymbol{b} Q' B^{c'} \Sigma^{-1} B^c Q \boldsymbol{b}' \tag{62}$$
$$= \sigma_\nu^2 \tag{63}$$

Note that the conditional likelihood of m_t does not depend on the full matrix B, but only on its first column, $\boldsymbol{b}$ because the model is partially identified. Therefore, we can rewrite (59) as

$$m_t|\boldsymbol{y}_t, \Pi, \Sigma, \boldsymbol{b}, \beta, \sigma_\nu \sim N(\mu_{m|Y}, V_{m|Y}), \tag{64}$$

Next, we can use the above result in a Metropolis step to generate a draw of $\boldsymbol{b}$: given a draw of Π, Σ, draw $Q_{\cdot,1}^{cand}$ as the first column of an orthogonal matrix form a uniform Haar distribution using the algorithm by Rubio-Ramirez et al. (2010). Set $Q_{\cdot,1} = Q_{\cdot,1}^{cand}$ with probability α and $Q_{\cdot,1}$ equal to the previous draw, $Q_{\cdot,1}^{j-1}$, otherwise.

$$\alpha = min(\frac{p(\boldsymbol{m}|Y, \Pi, \Sigma, Q_{\cdot,1}^{cand})}{p(\boldsymbol{m}|Y, \Pi, \Sigma, Q_{\cdot,1}^{j-1})}, 1)$$

Compute structural errors $\epsilon_{1,t} = (chol(\Sigma)Q_{\cdot,1})^{-1}U$.

A.5 Conditional posterior of β, σ_ν

Given a draw of structural shocks, $\epsilon_{1,t}$, the proxy equation is a linear equation. I consider two types of priors: a flat and a "high-relevance" prior. Restate the proxy equation for convenience

$$m_t = \beta \epsilon_{1,t} + \sigma_\nu \nu_t \tag{65}$$
$$\nu_t \sim N(0, 1), \tag{66}$$

First, for the flat prior, results from appendix A.2 apply and the normal-inverse

Gamma priors of the form

$$\beta \sim N(\mu_\beta^*, \sigma_\beta^{*2}) \tag{67}$$
$$\sigma_\nu^2 \sim IG(sc_\nu^*, sh_\nu^*) \tag{68}$$

map into posteriors of the form

$$\beta|\sigma_\nu \sim N(\mu_\beta, \sigma_\beta^2) \tag{69}$$
$$\sigma_\nu^2|\beta \sim IG(sc_\nu, sh_\nu) \tag{70}$$

with (assuming zero-centred un-informative priors)

$$\mu_\beta = \hat{\beta} \tag{71}$$
$$\sigma_\beta^2 = \sigma_\nu^2(\boldsymbol{\epsilon}_1\boldsymbol{\epsilon}_1')^{-1} \tag{72}$$
$$sc_\nu = T \tag{73}$$
$$sh_\nu = \hat{\nu}\hat{\nu}', \tag{74}$$

where $\hat{\nu}$ are the fitted errors from equation (65) and $\hat{\beta}$ is the OLS estimate of β.

Second, for the "high-relevance" prior, the posterior of β is unaffected. σ_ν, however, is not updated and stays at $\sigma_\nu = 0.5std(m_t)$ throughout the sampler.

A.6 Convergence of the Posterior Sampling Algorithm

The convergence properties of the reduced form parameters of a Bayesian FAVAR model are discussed in detail in Amir-Ahmadi and Uhlig (2015). They show that a Gibbs sampling procedure, similar to the one employed for the reduced form parameters here, converges for appropriate lengths of the sampler. The convergence properties of the structural parameters, however, need to be assessed. In particular the first column of B containing the on-impact effects of the shock of interest are of importance. In order to do so, I follow Amir-Ahmadi and Uhlig (2015) and employ the convergence diagnostic proposed by Geweke (1992). In addition, I compute inefficiency factors and the criterion by Raftery and Lewis (1992). A detailed discussion of these convergence diagnostics can be found, for example, in Cowles and Carlin (1996).

A.6.1 Geweke (1992)

The diagnostic by Geweke (1992) assesses the convergence of each element η_i of parameter vector, $\boldsymbol{\eta}$. The assessment is based on a comparison of means across different parts of this chain. If the means are close to each other, the procedure detects convergence.

In a first step, extract from each (univariate) posterior draw $\{\eta_i\}$ the following subseries: $\eta_{1i}, ..., \eta_{0.1D,i}$, i.e. the first 10 % of draws for parameter i, and $\eta_{0.6D+1,i}, ..., \eta_{D,i}$, i.e. the last 40% of draws, where D is the length of the MCMC chain. Compute $\hat{\mu}_{first}$ and $\hat{\mu}_{last}$, the mean, as well as $\hat{\sigma}_{first}$ and $\hat{\sigma}_{last}$, the standard deviation, of these subseries. Then the test statistic is

$$CD = \frac{\hat{\mu}_{first} - \hat{\mu}_{last}}{\frac{\hat{\sigma}_{first}}{\sqrt{0.1D}} + \frac{\hat{\sigma}_{last}}{\sqrt{0.4D}}} \tag{75}$$

Under the conditions mentioned in Geweke (1992), CD has an asymptotic standard normal distribution

The final output is a p-value indicating whether or not we can reject the Null hypothesis of convergence, i.e. equality of mean across the chain, at a given significance level.

A.6.2 Inefficiency Factors

Inefficiency factors are the inverse of the relative numerical efficiency measure (RNE) by Geweke (1992). The RNE assesses how many Gibbs draws should be used based on the autocorrelation of these draws. The RNE is computed noting that the posterior mean of a parameter η_i, $\mathbb{E}(\eta_i) = \frac{1}{N}\sum_{j=1}^{N} \eta_{i,j}$ would variance $\frac{\mathbb{E}(\eta_i)}{N}$ if the draws were generated independently. However, Gibbs draws are auto-correlated. That is why a variance estimate, which takes this auto-correlation into account, $S(0)/N$ (where $S(0)$ is the spectral density at frequency 0), will differ from $\frac{\mathbb{E}(\eta_i)}{N}$. The RNE is therefore given by:

$$RNE = \frac{\widehat{Var(\eta_i)}}{S(0)} \tag{76}$$

and inefficiency factors are defined as its inverse:

$$IF = RNE^{-1}. \tag{77}$$

A value of IF below 20, according to Primiceri (2005) indicates that the degree of autocorrelation is sufficiently low to indicate convergence of the posterior chain.

A.6.3 Raftery and Lewis (1992)

The approach by Raftery and Lewis (1992) investigates the quantiles of the probability distribution for the parameter η_i. The method assesses if the chain is long enough to get precise estimates of quantiles of this distribution.

To define the notion of closeness, three values have to be specified by the user: s, q and r. If the interest lies in $q_{i,0.025}$, the 0.025 quantile of the posterior of a parameter θ_i, then $q = 0.025$. If one exerts 95% of the posterior draws to lie in an interval of +/- 0.0125 around the true 0.025 quantile, then $s = 0.95$ and $r = 0.0125$. These specifications are standard for output from an MCMC chain. The implementation of the algorithm for each parameter j proceeds in 4 steps:

1. transform $\{\eta_{i,d}\}_{d=1}^{D}$ into a dichotomous random variable Z_d:

$$Z_d = \begin{cases} 1 & \text{if } \eta_{i,d} < q_{0.025}, \\ 0 & \text{otherwise;} \end{cases} \tag{78}$$

2. write the matrix of transition probabilities for Z_d conditioning on the previous state,

$$\mathcal{P} = \begin{bmatrix} 1-\alpha & \alpha \\ \beta & 1-\beta \end{bmatrix},$$

with $\alpha = P(Z_{d+1} = 1|Z_d = 0)$ and $\beta = P(Z_{d+1} = 0|Z_d = 1)$. The unconditional probabilities of being in one state or another are

$$\pi_0 = P(\eta_{i,d} < q_{0.025}) = P(Z_d = 0) = \frac{\beta}{\alpha + \beta} \tag{79}$$

$$\pi_1 = P(\eta_{i,d} \geq q_{0.025}) = P(Z_d = 1) = 1 - \pi_0 = \frac{\alpha}{\alpha + \beta} \tag{80}$$

3. approximate the probability that a draw of the parameter is smaller than the quantile of interest as

$$P(\eta_{i,d} < q_{0.025}) \approx \bar{Z}_{D,i} = \frac{1}{D} \sum_{d=1}^{D} Z_d. \tag{81}$$

As shown by Raftery and Lewis (1992), $\bar{Z}_D$ is approximately normally distributed with mean $q_{0.025}$ and variance $\frac{1}{D}\frac{(2-\alpha-\beta)\alpha\beta}{(\alpha+\beta)^3}$;

4. compute the optimal length of the chain as the length that ensures $P(q - r \leq$

$\bar{Z}_D \leq q + r$) using

$$n^* = \frac{(2-\alpha-\beta)\alpha\beta}{(\alpha+\beta)^3}\left\{\frac{\Phi^{-1}(\frac{1}{2}(s+1))}{r}\right\}^2 \tag{82}$$

The key statistic of the test is n^*, which has an intuitive interpretation: it is the minimum number of draws we need for the desired level of accuracy of the quantile q (given by r and s). If the number of draws, D, is lower than n^*, this suggests that the chain length needs to be increased.

B Deviance Information Criterion

This section lays out how to employ the deviance information Criterion (DIC) by Spiegelhalter et al. (2002) to determine the number of latent factors, R, used in the analysis. I employ the DIC rather than measures of marginal data densities (MDD) since, as pointed out by Chan and Eisenstat (2018), the MDD, while having an intuitive interpretation, tends to be more sensitive to the choice of priors and comes with a heavy computational burden. The DIC is given as:

$$DIC = \overline{D(\theta)} + p_D, \tag{83}$$

where

$$\overline{D(\theta)} = -2\mathbb{E}_{\theta,F}(\log\, p(Z|\theta, F)|Z) \tag{84}$$

is the posterior mean deviance, interpreted as the residual information in the data conditional on θ (see e.g. Chan and Eisenstat, 2018 for a discussion) and $p(Z|\theta, F)$ is the likelihood conditional on latent factors. It is calculated by averaging $-2\log\, p(Z|\theta, F)$ across posterior draws. Next,

$$p_D = \overline{D(\theta)} - D(\tilde{\theta}) \tag{85}$$

is the effective number of parameters in the model, a measure of shrinkage of the posterior estimates towards the prior means (Chan and Eisenstat, 2018). $\tilde{\theta}$ is chosen as the posterior mean of parameters and the Principal Components estimate of latent factors. The preferred model is the one with the minimum DIC value.

The DIC in this paper is based on a measure of the conditional likelihood, $p(Z|\theta, F)$, rather than the full-data likelihood $p(Z|\theta)$. Monte Carlo evidence by Chan and Grant (2016) suggests that this variant of the DIC tends to favour complex models. However, this procedure is widely used in applied work (see e.g. Mumtaz and Surico, 2012, Yu and Meyer, 2006) since the conditional likelihood is often available in closed form and therefore straightforward to implement.

C Numerical Illustration

This section lays out the simulation design in section 3.3 of the paper.

C.1 Data Generating Process

Data are generated from a Proxy-FAVAR using two data generating processes (DGP). The parameters are given in table 2. DGP1 uses a non-contaminated proxy to abstract from the challenges of measurement errors in the proxy. DGP2 introduces a contamination, lowering β_{true} and increasing $\sigma_{\nu,true}$.

	$\boldsymbol{\beta}_{true}$	$\boldsymbol{\sigma}_{\nu,true}$	**R**	**K**	**N**	**T**	**repl.**	**draws**	**burn-in**
DGP1	1	0	3	1	9	200	50	25,000	5,000
DGP2	0.5	1							

Table 2: ***Numerical Illustration: DGP.*** *Parameters used to generate artificial data.*

The remaining parameters are set as follows:

$$\Lambda_{true} = \begin{bmatrix} 1.20 & 0.30 & 0.10 & 0.00 \\ 0.54 & 2.21 & -1.04 & 0.00 \\ 0.41 & 0.52 & 2.29 & 0.00 \\ -1.19 & -0.92 & 0.23 & 0.50 \\ 1.19 & -0.12 & 0.31 & 0.30 \\ -1.14 & 0.13 & 0.43 & 0.00 \\ 1.14 & -0.96 & 0.25 & 0.00 \\ -0.67 & 1.28 & 1.41 & 0.00 \\ 1.08 & -0.56 & 0.52 & 0.00 \end{bmatrix}, \Omega_{true} = diag(\begin{bmatrix} 0.01 \\ 0.01 \\ 0.01 \\ 0.01 \\ 0.01 \\ 0.01 \\ 0.01 \\ 0.01 \\ 0.01 \end{bmatrix}), b_{true} = \begin{bmatrix} 1 \\ 0.1 \\ -0.2 \\ 0.3 \end{bmatrix}$$

$$\Pi_{true} = \begin{bmatrix} 0.8 & 0 & 0 & 0 \\ 0 & 0.75 & 0 & 0 \\ 0 & 0 & 0.7 & 0 \\ 0 & 0 & 0 & 0.5 \end{bmatrix}, \Sigma_{true} = \begin{bmatrix} 0.92 & 0.06 & 0.01 & 0.09 \\ 0.06 & 1.23 & -0.14 & -0.12 \\ 0.01 & -0.14 & 1.13 & 0.08 \\ 0.09 & -0.12 & 0.08 & 0.95 \end{bmatrix}$$

The parameter values chosen for Λ_{true} ensure that $\Lambda^{f\prime}_{true}\Lambda^{f}_{true} = I_R$, and the top $(R \times K)$ block of Λ_{true} is zero, satisfying the normalisation used for factors and factor loadings (see section 2). The data are generated using the following steps:

Data Generating Process (DGP)

1. Draw $2T$ reduced form shocks $\boldsymbol{u}_t$ from $N(\mathbf{0}, \tilde{\Sigma}_{true})$.

2. Generate factors $\boldsymbol{y}_t$ recursively using Π_{true} and $\boldsymbol{u}_t$, starting from $\boldsymbol{y}_1 = \mathbf{0}$. Discard the first T observations to limit the effect of starting values.

3. Set the non-normalised latent factors to $\tilde{\boldsymbol{f}}_{t,true} = \boldsymbol{y}_{t,1:R}$. Recover the normalised factors, $\boldsymbol{f}_{t,true}$, with $cov(\boldsymbol{f}_t)$ diagonal with decreasing elements. Set the observable factor to $z_t = \boldsymbol{y}_{t,R+1}$. Recover $\boldsymbol{u_t} = [\boldsymbol{f}_{t,true} \quad z_t]' - \Pi_{true}[\boldsymbol{f}_{t-1,true} \quad z_{t-1}]'$ and $\Sigma_{true} = \sum_{t=1}^{T} \boldsymbol{u_t}\boldsymbol{u_t}'/T$.

4. Recover $\epsilon_{1,t} = b'_{true}\Sigma^{-1}_{true}\boldsymbol{u}_t/(b'_{true}\Sigma^{-1}_{true}b_{true})$ and generate the proxy $m_t = \beta_{true}\epsilon_{1,t} + \nu_t$, with $\nu_t \sim N(0, \sigma^2_{\nu,true})$

5. Generate informational series $\tilde{\boldsymbol{x}}_t = \Lambda_{true}[\boldsymbol{f}_{t,true} z_t]' + \boldsymbol{\xi}_t$, where $\xi_t \sim N(\mathbf{0}, \Omega_{true})$. Standardise the informational series, setting $x_t = (\tilde{\boldsymbol{x}}_{\boldsymbol{t}} - \sum_{t=1}^{T} \tilde{\boldsymbol{x}}_t/T)/std(\tilde{\boldsymbol{x}}_{\boldsymbol{t}})$.

50 data sets are generated. For each data set, 25,000 posterior draws from the BP-FAVAR model are generated, discarding the first 5,000. The parameter draws are pooled across simulations. While the posterior draws of parameters can be compared to their true values, the true factors differ for each simulation so that their posterior draws cannot be compared to their true counterpart.

D Additional Figures and Tables

D.1 Sampler Specification

	DGP1	DGP2	Mon. Pol. (1)	Mon. Pol. (2)	Oil Mkt.
Total nb of draws	25,000	25,000	100,000	100,000	100,000
burn-in	5,000	5,000	10,000	10,000	10,000
acc. red. form	0.995	0.802	0.976	0.941	0.975
acc. Q	0.02	0.182	0.046	0.153	0.076

Table 3: ***Sampler Specification.*** *Effective number of draws are the total number minus the burn-in sample. The reduced form acceptance rate refers to the Metropolis-Hastings step in step 3 of the sampler. The acceptance rate for Q refers to the Metropolis-Hastings step in step 4 of the sampler. DGP1 and DGP2 refer to the two data-generating processes used in the numerical application Mon. Pol. (1) and (2) refer to the application to monetary policy shocks using the proxy by Caldara and Herbst (2019) and Miranda-Agrippino and Ricco (2018), respectively. The last column refers to the oil market application.*

D.2 Additional Results for Numerical Illustration

	DGP1			DGP2		
	G1992	RL1991	Ineff.Fac.	G1992	RL1991	Ineff.Fac.
$\boldsymbol{f_1}$	0.19	16,656.41	7.80	0.14	32,412.42	11.16
$\boldsymbol{f_2}$	0.00	9,881.11	16.93	0.39	17,610.89	13.35
$\boldsymbol{f_3}$	0.34	5,618.40	13.14	0.94	12,704.67	13.12
$\mathbf{z}$	0.06	4,767.12	12.30	0.13	8,034.91	10.94

Table 4: ***Numerical Illustration: Convergence.*** *Convergence criteria for the impact effect of factors, $\mathbf{b}$. G1992 is the p-value of the criterion by Geweke (1992). A p-value above 0.01 suggests that the Null hypothesis of convergence cannot be rejected at the 1% confidence level. RL1992 is the minimum number of draws required for convergence as proposed by Raftery and Lewis (1992). Ineff. Fac. are inefficiency factors, as in Primiceri (2005). A value below 20 suggests convergence. The sampler ran for 25,000 draws, discarding the first 5,000 draws as a burn-in sample.*

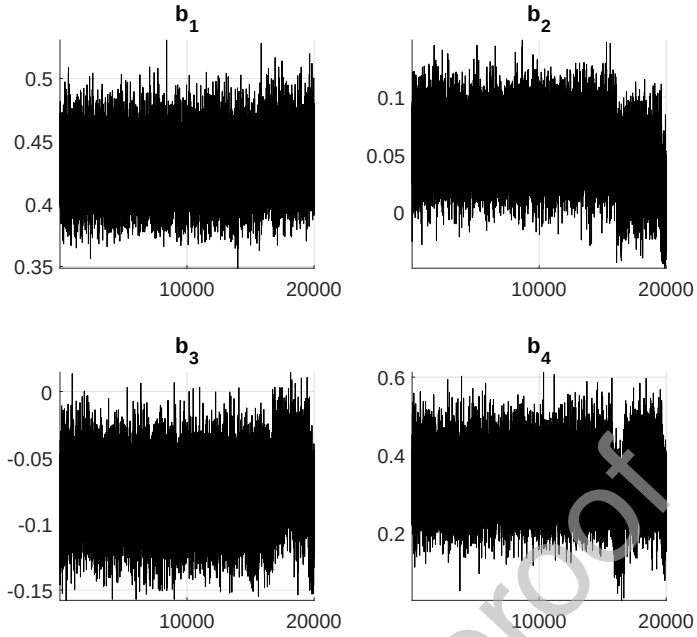

(a) DGP1

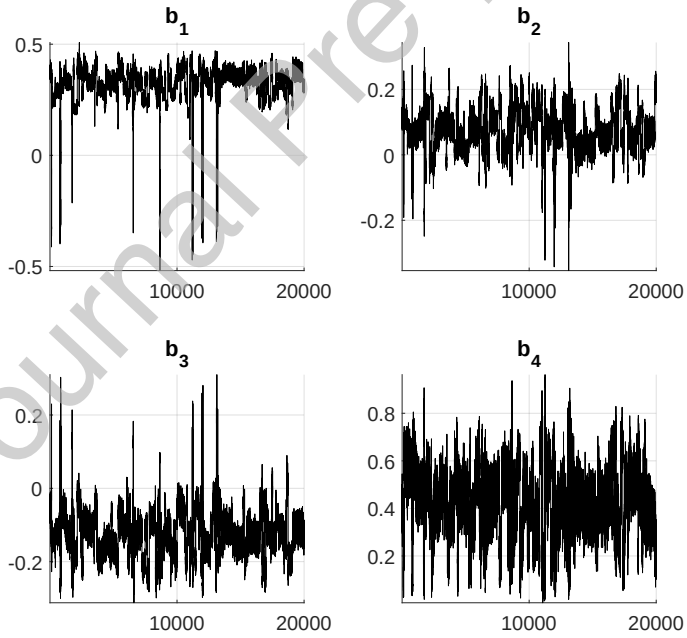

(b) DGP2

Numerical Illustration: Posterior Draws. *Draws from the posterior of* $\mathbf{b}$ *for DGP1 (top panel) and DGP2 (bottom panel). Draws after the burn-in sample are plotted.*

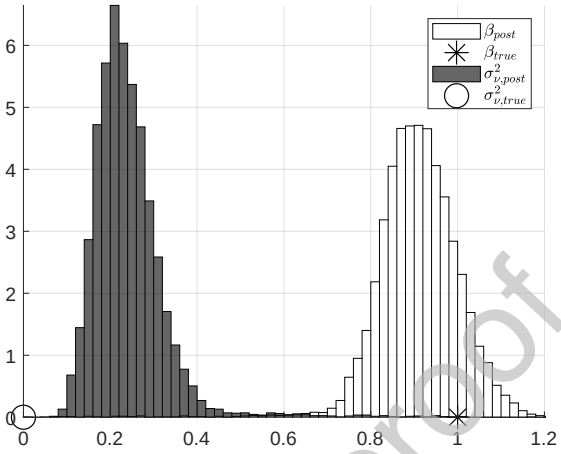

(a) DGP1

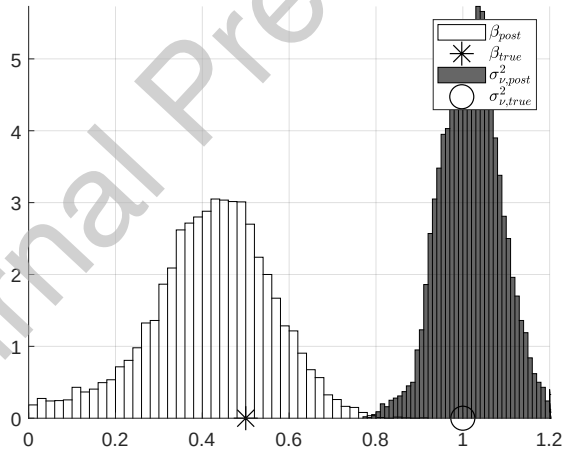

(b) DGP2

(c) ***Numerical Illustration:*** β ***and*** σ^2_ν***.*** *Posterior draws of* β *and* σ_ν *and true values for DGP1 (top panel) and DGP2 (bottom panel)*

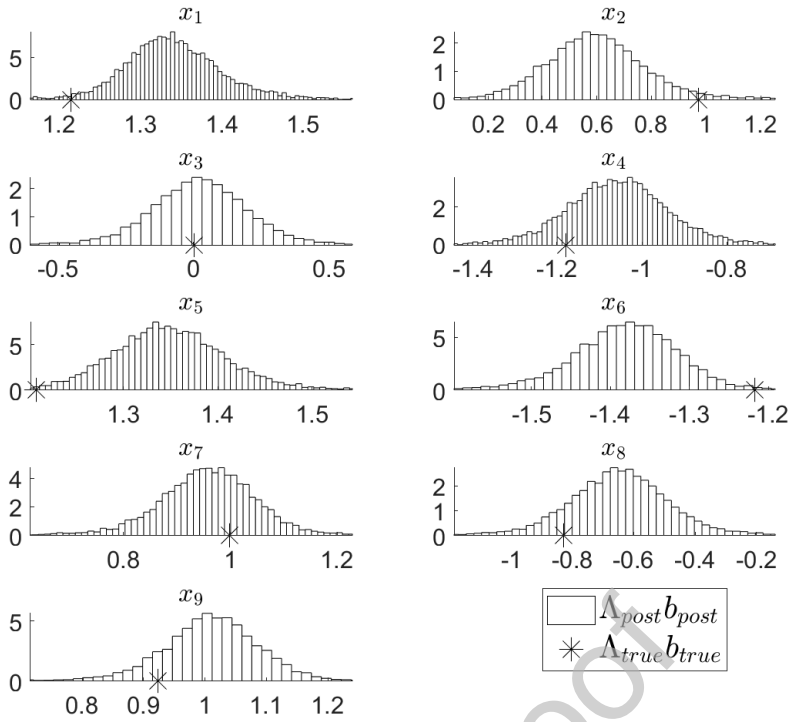

(a) DGP1

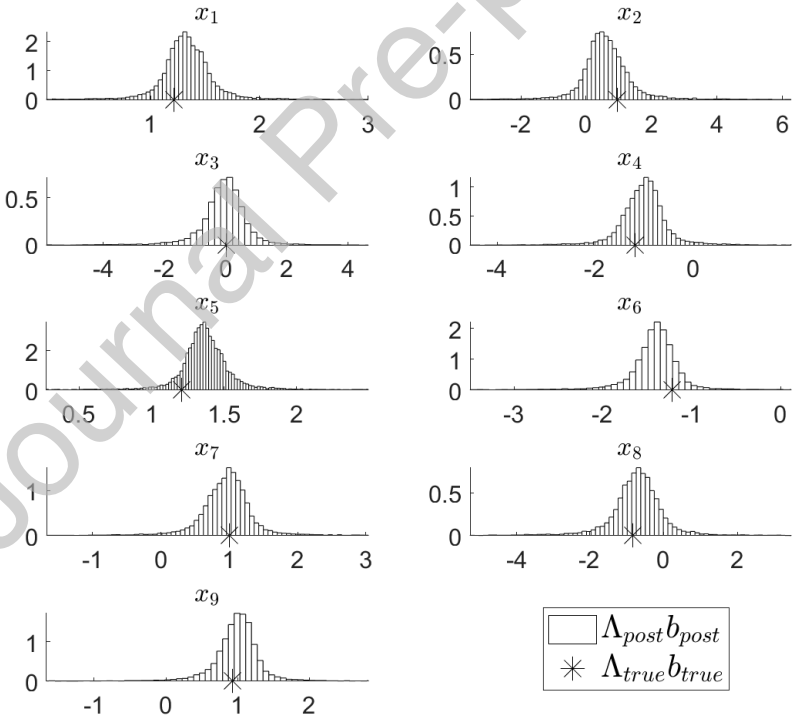

(b) DGP2

Figure 11: ***Numerical Illustration: Impact Effects.*** *Posterior draws of the impact effects of informational series, $\Lambda_{post} b_{post}$ and corresponding true values for DGP1 (top panel) and DGP2 (bottom panel)*

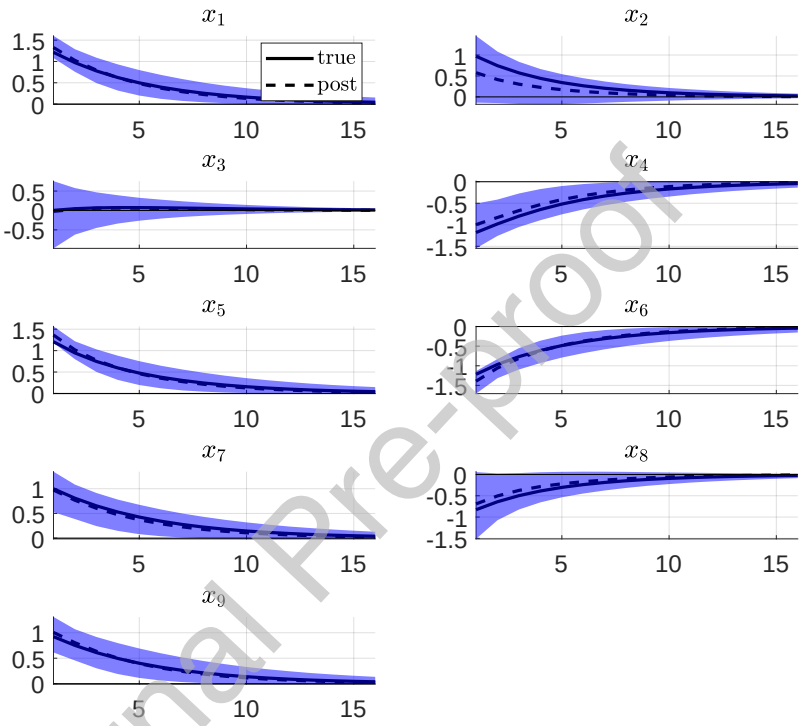

Figure 12: ***Numerical Illustration: Impulse Responses (DGP2).*** *Posterior draws of the impulse responses of informational series, and corresponding true values for DGP2. The shaded area shows 80% quantiles of posterior draws pooled across simulations. The dashed line is the posterior median, while the solid line is the true impulse response.*

D.3 Additional Results for Monetary Policy Application

D.3.1 Baseline: Caldara and Herbst (2019) Proxy

b	G1992	RL1991	Ineff. Fac.
1	0.76	53,713.33	25.50
2	0.51	15,121.60	11.45
3	0.52	11,831.04	9.02
4	0.06	12,557.33	9.29
5	0.84	17,486.08	11.13

Table 5: ***Monetary Policy Application (Caldara and Herbst, 2019): Convergence.*** *Convergence criteria for the impact effect of factors,* **b**. *G1992 is the p-value of the criterion by Geweke (1992). A p-value above 0.01 suggests that the Null hypothesis of convergence cannot be rejected at the 1% confidence level. RL1992 is the minimum number of draws required for convergence as proposed by Raftery and Lewis (1992). The last column reports inefficiency factors, as in Primiceri (2005). A value below 20 suggests convergence. The sampler ran for 100,000 draws.*

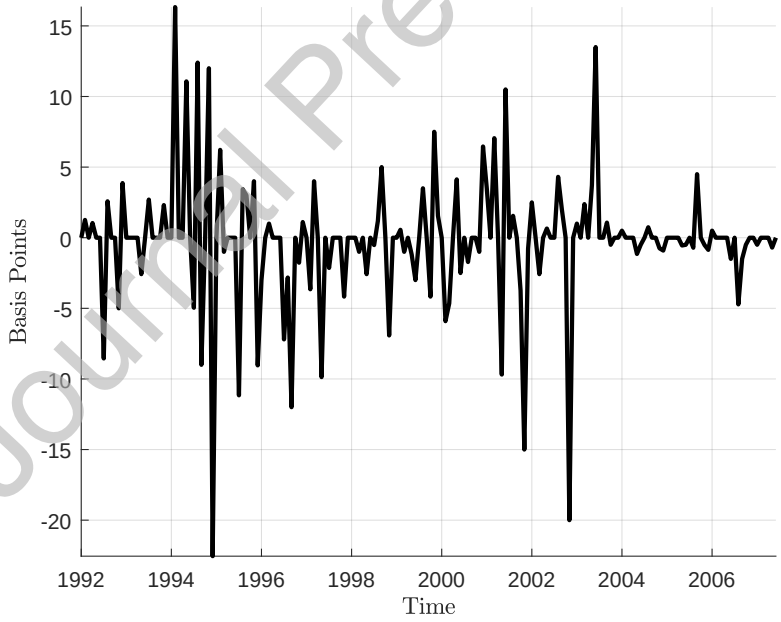

Figure 13: ***Proxy for monetary policy shocks.*** *Monetary policy surprises associated with FOMC announcements. The methodology uses the price of federal funds future contracts traded at the Chicago Board of Trade. See Caldara and Herbst (2019) for details.*

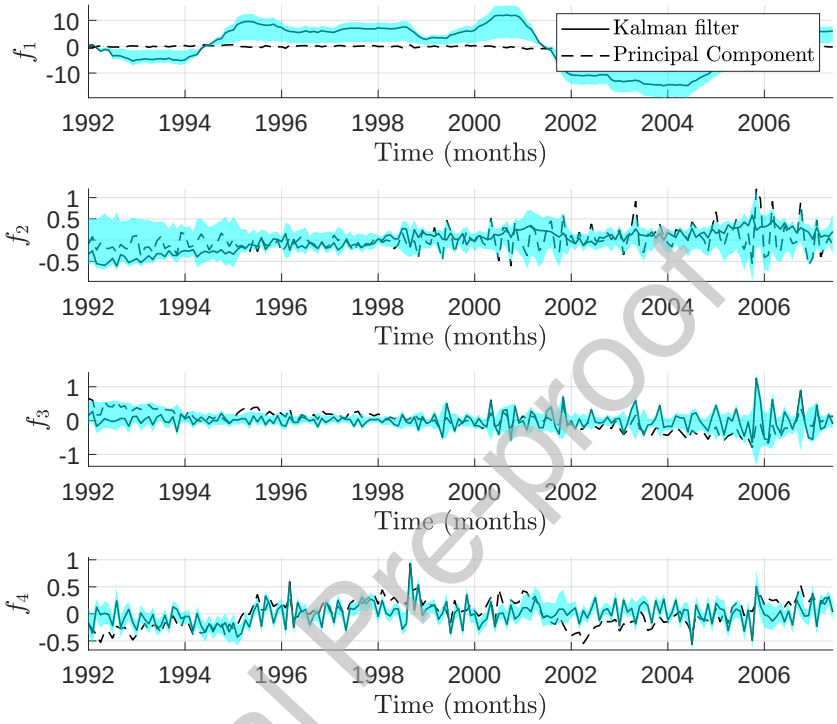

Figure 14: ***Posterior of latent factors (monetary policy application).*** *Median posterior draw of latent factors estimated via Kalman filter (solid line). 90% bands (dotted) and Principal Components estimate (dashed).*

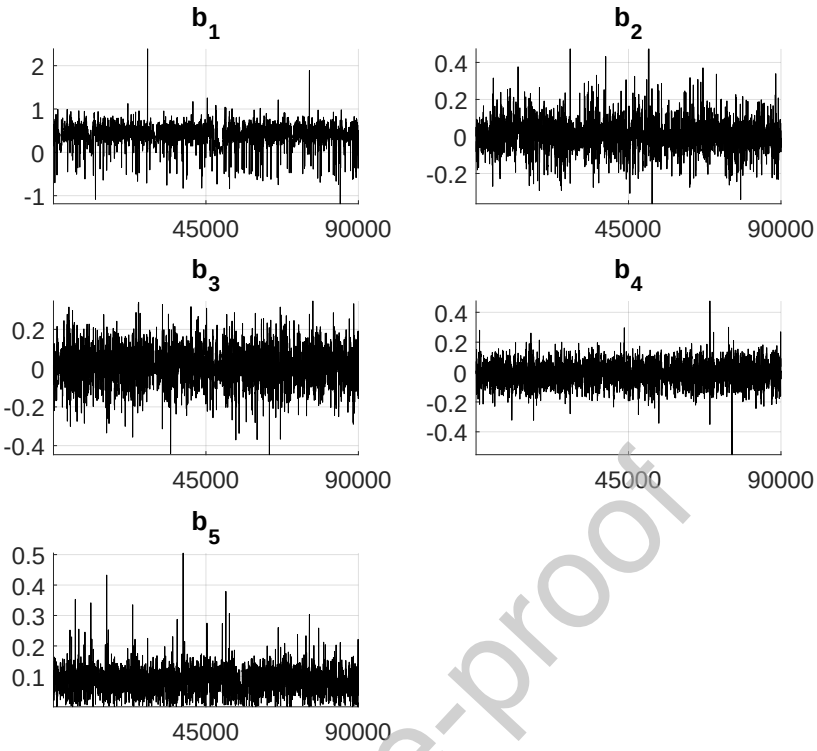

Figure 15: ***Monetary Policy Application (Caldara and Herbst, 2019): Posterior Draws.*** *Draws from the posterior of* $\mathbf{b}$*. Draws after the burn-in sample are plotted.*

D.3.2 High-relevance Prior

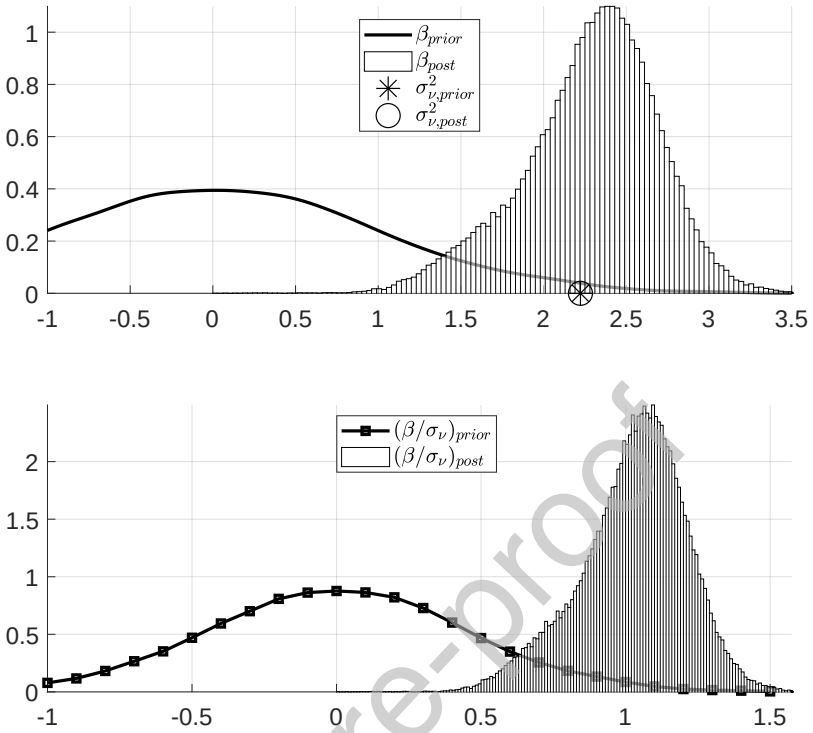

Figure 16: ***Monetary Policy Application (High-relevance prior): Instrument Relevance.*** *Top panel: Update of β and σ^2_ν. The prior for β is standard normal, while the prior for σ^2_ν imposes $\sigma_\nu = 0.5std(m_t)$. The proxy by Caldara and Herbst (2019) is used for identification.*

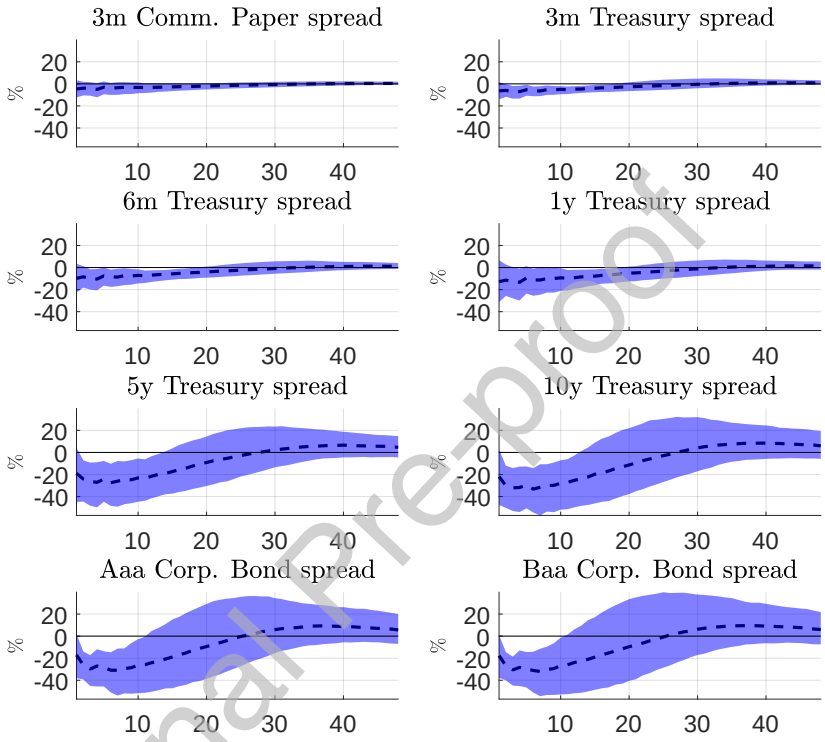

Figure 17: ***Monetary Polcy Application (High-relevance prior): Impulse Response Functions of informational series.*** *Point-wise median impulse responses (solid line) with 68% bands. The model includes $R = 4$ latent factors from real and financial series. The impact effect is normalised to generate a 0.25% increase in the observable factor. The proxy by Caldara and Herbst (2019) is used for identification. The prior for σ_ν imposes $\sigma_\nu = 0.5std(m_t)$.*

D.3.3 Miranda-Agrippino and Ricco (2018) Proxy

b	G1992	RL1991	Ineff. Fac.
1	0.48	21,267.04	11.59
2	0.77	14,844.15	20.45
3	0.79	12,525.05	3.26
4	0.35	12,240.15	3.59
5	0.83	9,861.97	3.55

Table 6: ***Monetary Policy Application (Miranda-Agrippino and Ricco, 2018): Convergence.*** *Convergence criteria for the impact effect of factors,* ***b****. G1992 is the p-value of the criterion by Geweke (1992). A p-value above 0.01 suggests that the Null hypothesis of convergence cannot be rejected at the 1% confidence level. RL1992 is the minimum number of draws required for convergence as proposed by Raftery and Lewis (1992). The last column reports inefficiency factors, as in Primiceri (2005). A value below 20 suggests convergence. The sampler ran for 100,000 draws.*

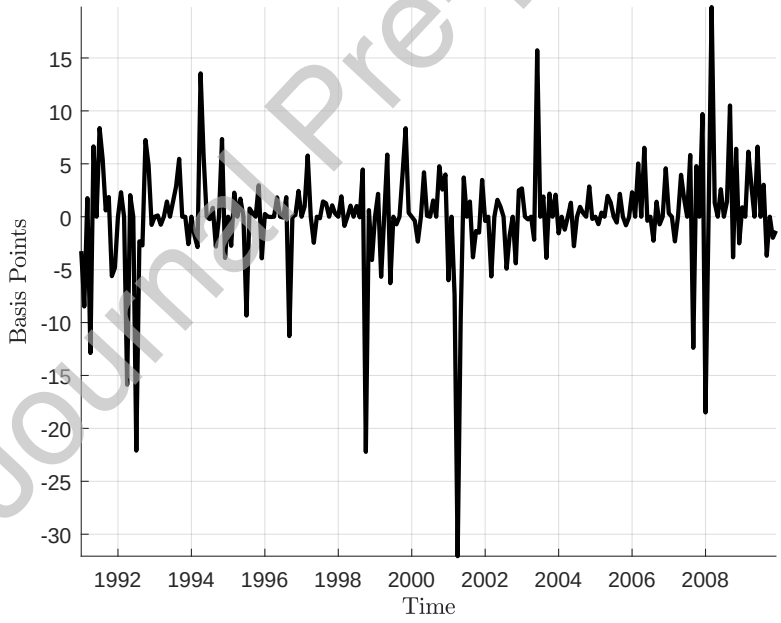

Figure 18: ***Monetary Policy Application (Miranda-Agrippino and Ricco, 2018): Proxy.*** *Monetary policy surprises accounting for informational rigidities. See Miranda-Agrippino and Ricco (2018) for details.*

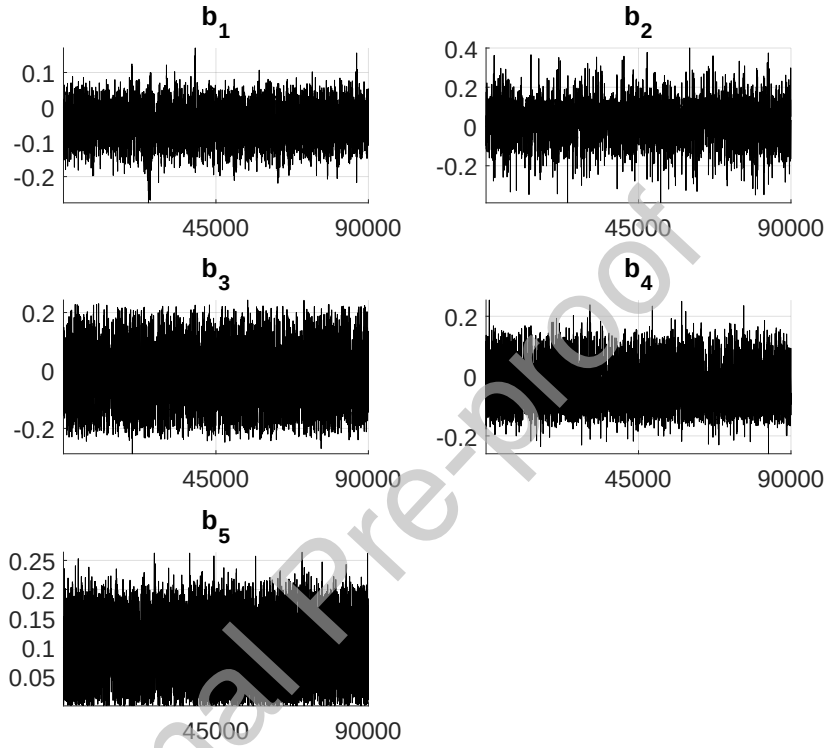

Figure 19: ***Monetary Policy Application (Miranda-Agrippino and Ricco, 2018): Posterior Draws.*** *Draws from the posterior of* $\mathbf{b}$*. Draws after the burn-in sample are plotted.*

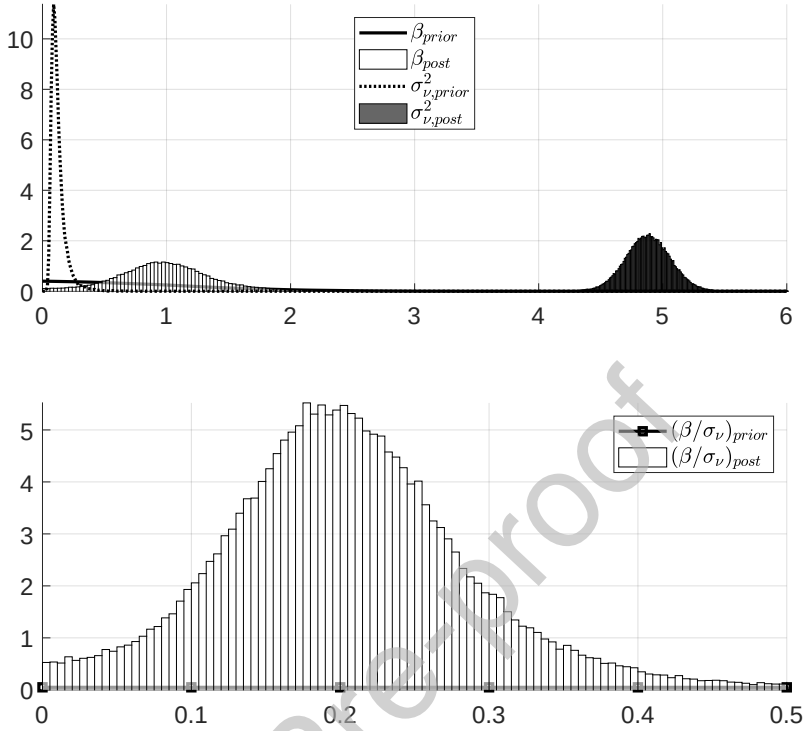

Figure 20: ***Monetary Policy Application (Miranda-Agrippino and Ricco, 2018):Instrument Relevance.*** *Top panel: Update of β and σ^2_ν. The prior for β is standard normal, while the prior for σ^2_ν follows an inverse Gamma distribution. Bottom panel: Update of β/σ_ν.*

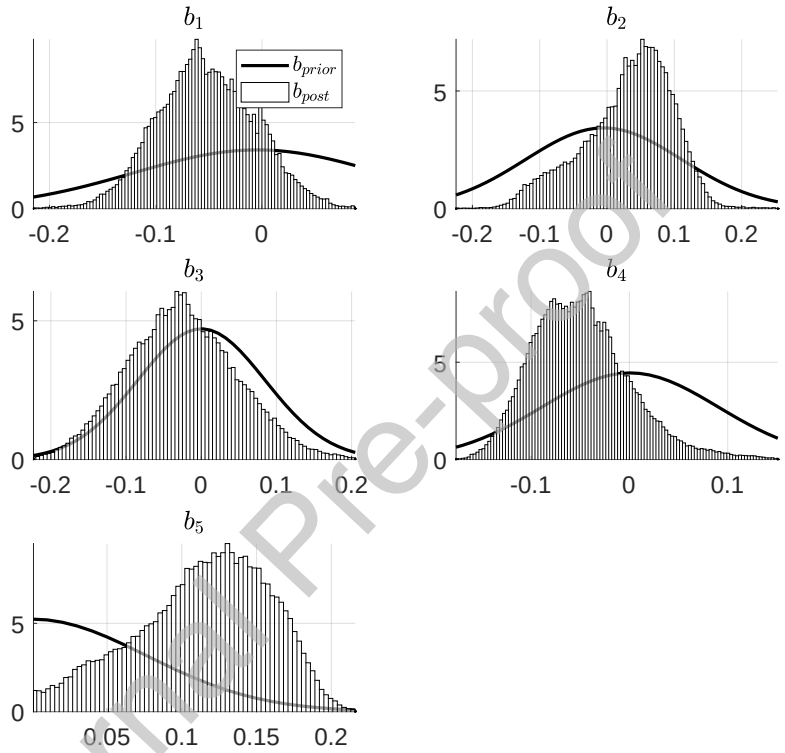

Figure 21: ***Monetary Policy Application (Miranda-Agrippino and Ricco, 2018): Updating of b.*** *Priors (solid line) and posterior (histogram) of* $\mathbf{b}$*. Prior draws are computed from the distribution implicit in the priors for* Σ*,* β *and* σ_ν*.*

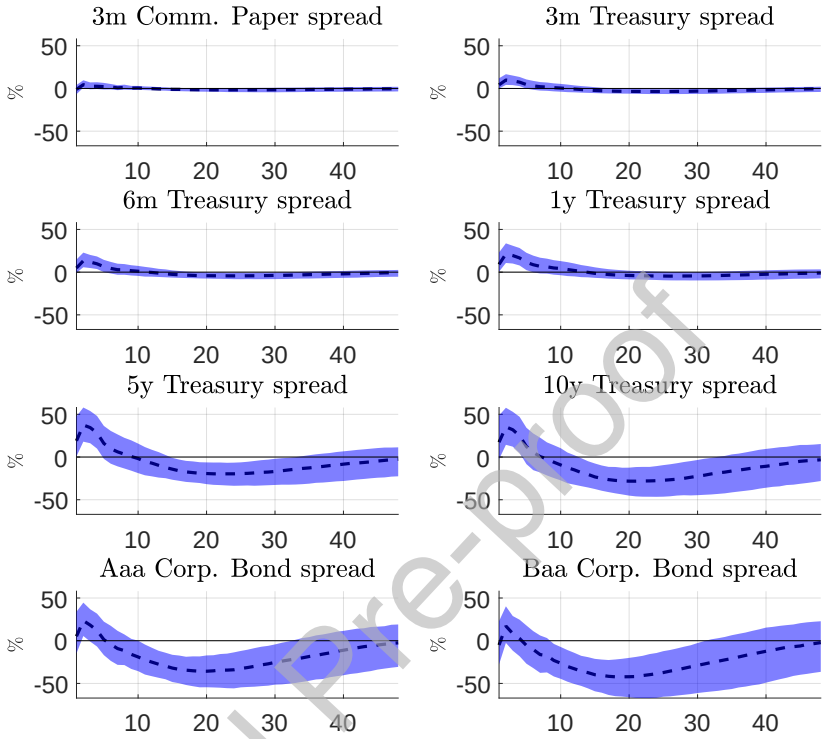

Figure 22: ***Monetary Policy Application (Miranda-Agrippino and Ricco, 2018): Impulse Response Functions of informational series.*** *Point-wise median impulse responses (solid line) with 68% bands. The model includes $R = 4$ latent factors from real and financial series. The impact effect is normalised to generate a 0.25% increase in the observable factor. The proxy by Miranda-Agrippino and Ricco (2018) is used for identification*

D.4 Oil Market Application

R	DIC
1	5497.12
2	-4942.12
3	**-67,529.90**
4	-14,996.23
5	-20,457.62
6	-9032.89
7	-12,198.27
8	-14,238.08

Table 7: ***Deviance Information Criterion (Oil application).*** *Deviance Information Criterion (DIC) by Spiegelhalter et al. (2002). The preferred model minimises the DIC. The sampler is run $R_{max} = 8$ times for 20,000 draws, discarding the first 2,000 draws. See Appendix B for details.*

b	G1992	RL1991	Ineff. Fac.
1	0.47	28,163.69	11.89
2	0.34	25,312.01	12.50
3	0.89	20,636.16	9.82
4	0.60	24,538.90	12.29
5	0.55	25,391.44	11.62
6	0.55	17,991.59	17.34
7	0.33	22,339.00	10.90

Table 8: ***Oil market application: Convergence.*** *Convergence criteria for the impact effect of factors, **b**. G1992 is the p-value of the criterion by Geweke (1992). A p-value above 0.01 suggests that the Null hypothesis of convergence cannot be rejected at the 1% confidence level. RL1992 is the minimum number of draws required for convergence as proposed by Raftery and Lewis (1992). The last column reports inefficiency factors, as in Primiceri (2005). A value below 20 suggests convergence. The sampler ran for 100,000 draws, discarding the first 10,000 draws.*

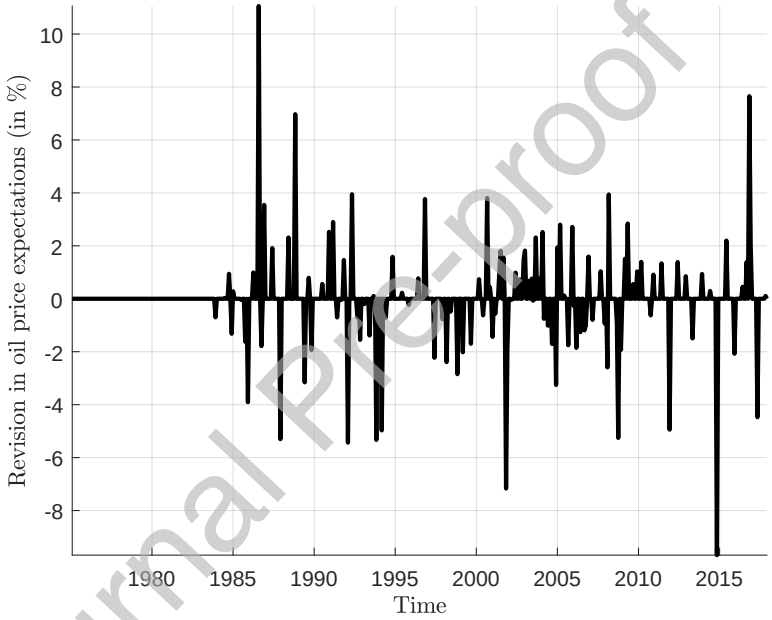

Figure 23: ***Proxy for oil supply news shocks.*** *Percent variation in WTI oil price futures around OPEC announcements, see Känzig (2019).*

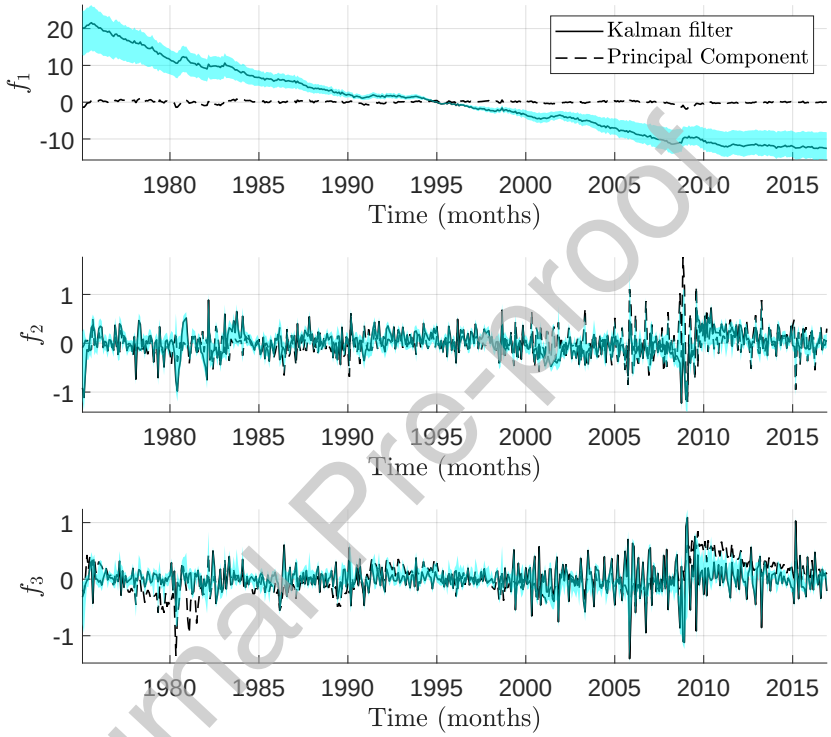

Figure 24: ***Posterior of latent factors (oil market application).*** *Median posterior draw of latent factors estimated via Kalman filter (solid line). 90% bands (dotted) and Principal Components estimate (dashed).*

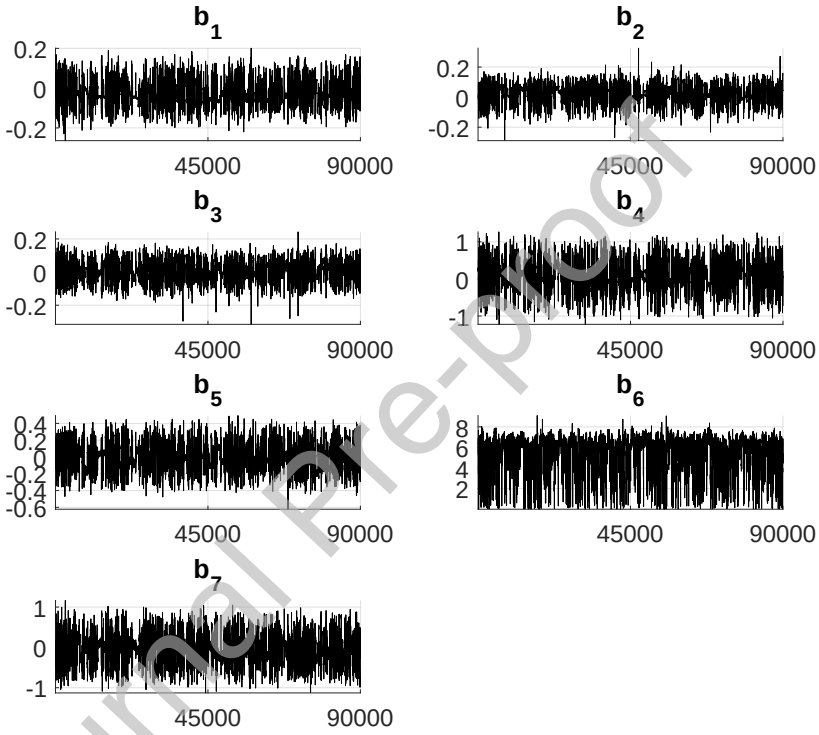

Figure 25: ***Oil market Application: Posterior Draws.*** *Draws from the posterior of* $\mathbf{b}$*. Draws after the burn-in sample are plotted.*

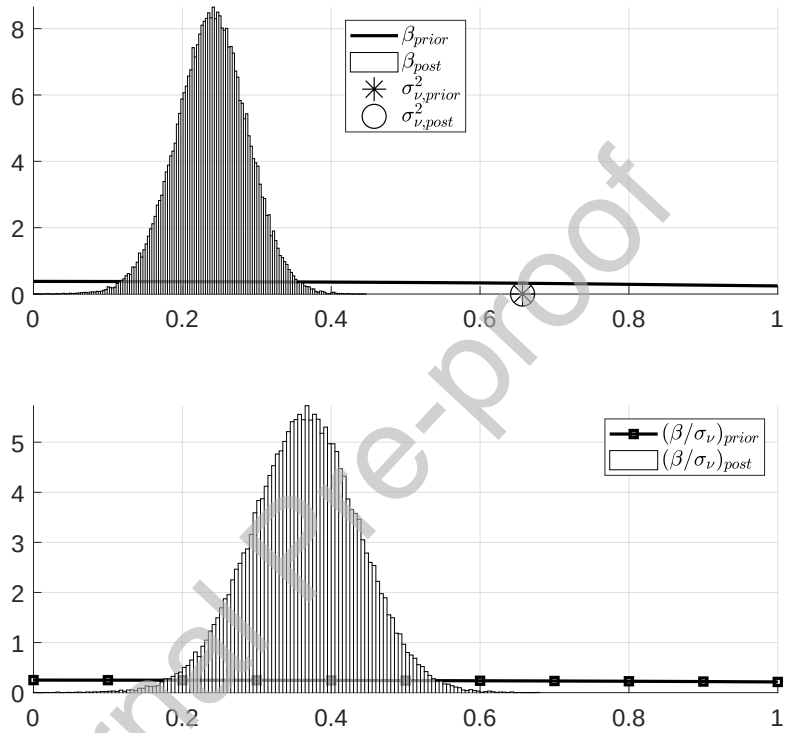

Figure 26: ***Oil Market Application (high relevance prior): Instrument Relevance.*** *Top panel: Update of β and σ^2_ν. The prior for β is standard normal, while the prior for σ^2_ν imposes $\sigma_\nu = 0.5std(m_t)$.*

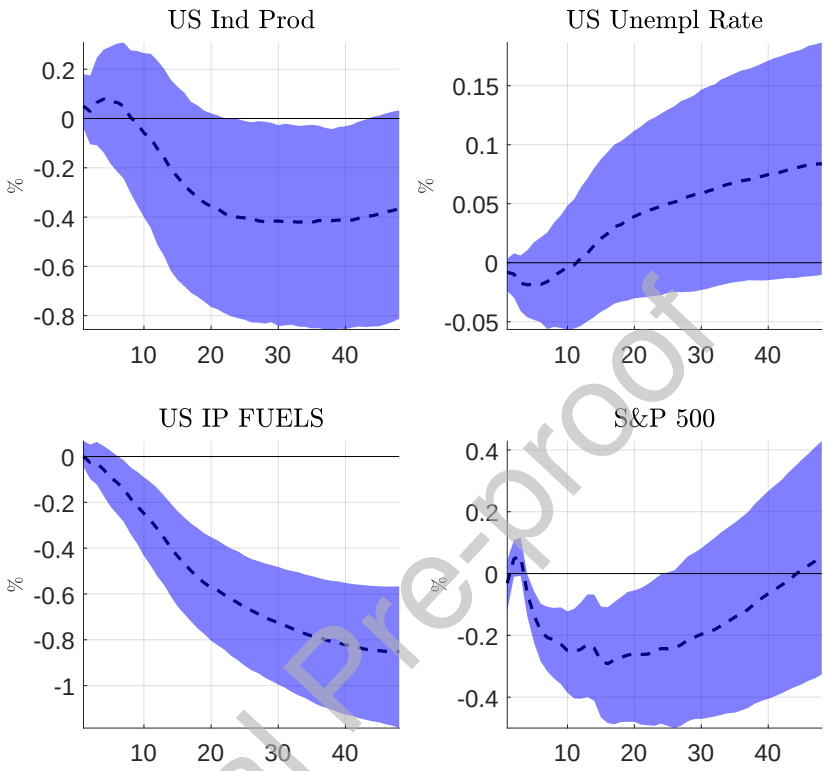

Figure 27: ***Impulse Response Functions of informational series (Oil market application, high relevance prior).*** *Point-wise median impulse responses (solid line) with 68% bands. The model includes $R = 3$ latent factors. The impact effect is normalised to generate a 7% increase in the WTI spot price. The proxy by Känzig (2019) is used for identification. The prior for β is standard normal, while the prior for σ_ν^2 imposes $\sigma_\nu = 0.5std(m_t)$.*

Table 9: Data

Output and Income

id	tcode	fred	description
1	5	RPI	Real Personal Income
2	5	W875RX1	Real personal income ex transfer receipts
6	5	INDPRO	IP Index
7	5	IPFPNSS	IP: Final Products and Nonindustrial Supplies
8	5	IPFINAL	IP: Final Products (Market Group)
9	5	IPCONGD	IP: Consumer Goods
10	5	IPDCONGD	IP: Durable Consumer Goods
11	5	IPNCONGD	IP: Nondurable Consumer Goods
12	5	IPBUSEQ	IP: Business Equipment
13	5	IPMAT	IP: Materials
14	5	IPDMAT	IP: Durable Materials
15	5	IPNMAT	IP: Nondurable Materials
16	5	IPMANSICS	IP: Manufacturing (SIC)
17	5	IPB51222s	IP: Residential Utilities
18	5	IPFUELS	IP: Fuels
19	1	NAPMPI	ISM Manufacturing: Production Index
20	2	CUMFNS	Capacity Utilization: Manufacturing

Labor Market			
id	tcode	fred	description
21*	2	HWI	Help-Wanted Index for United States
22*	2	HWIURATIO	Ratio of Help Wanted/No. Unemployed
23	5	CLF16OV	Civilian Labor Force
24	5	CE16OV	Civilian Employment
25	2	UNRATE	Civilian Unemployment Rate
26	2	UEMPMEAN	Average Duration of Unemployment (Weeks)
27	5	UEMPLT5	Civilians Unemployed - Less Than 5 Weeks
28	5	UEMP5TO14	Civilians Unemployed for 5-14 Weeks
29	5	UEMP15OV	Civilians Unemployed - 15 Weeks & Over
30	5	UEMP15T26	Civilians Unemployed for 15-26 Weeks
31	5	UEMP27OV	Civilians Unemployed for 27 Weeks and Over
32*	5	CLAIMSx	Initial Claims
33	5	PAYEMS	All Employees: Total nonfarm
34	5	USGOOD	All Employees: Goods-Producing Industries
35	5	CES1021000001	All Employees: Mining and Logging: Mining
36	5	USCONS	All Employees: Construction
37	5	MANEMP	All Employees: Manufacturing
38	5	DMANEMP	All Employees: Durable goods
39	5	NDMANEMP	All Employees: Nondurable goods
40	5	SRVPRD	All Employees: Service-Providing Industries
41	5	USTPU	All Employees: Trade, Transportation & Utilities
42	5	USWTRADE	All Employees: Wholesale Trade
43	5	USTRADE	All Employees: Retail Trade
44	5	USFIRE	All Employees: Financial Activities
45	5	USGOVT	All Employees: Government
46	1	CES0600000007	Avg Weekly Hours : Goods-Producing
47	2	AWOTMAN	Avg Weekly Overtime Hours : Manufacturing
48	1	AWHMAN	Avg Weekly Hours : Manufacturing
49	1	NAPMEI	ISM Manufacturing: Employment Index
127	6	CES0600000008	Avg Hourly Earnings : Goods-Producing
128	6	CES2000000008	Avg Hourly Earnings : Construction
129	6	CES3000000008	Avg Hourly Earnings : Manufacturing

Housing			
id	tcode	fred	description
50	4	HOUST	Housing Starts: Total New Privately Owned
51	4	HOUSTNE	Housing Starts, Northeast
52	4	HOUSTMW	Housing Starts, Midwest
53	4	HOUSTS	Housing Starts, South
54	4	HOUSTW	Housing Starts, West
55	4	PERMIT	New Private Housing Permits (SAAR)
56	4	PERMITNE	New Private Housing Permits, Northeast (SAAR)
57	4	PERMITMW	New Private Housing Permits, Midwest (SAAR)
58	4	PERMITS	New Private Housing Permits, South (SAAR)
59	4	PERMITW	New Private Housing Permits, West (SAAR)
Consumption, Orders and inventories			
3	5	DPCERA3M086SBEA	Real personal consumption expenditures
4*	5	CMRMTSPLx	Real Manu. and Trade Industries Sales
5*	5	RETAILx	Retail and Food Services Sales
60	1	NAPM	ISM : PMI Composite Index
61	1	NAPMNOI	ISM : New Orders Index
62	1	NAPMSDI	ISM : Supplier Deliveries Index
63	1	NAPMII	ISM : Inventories Index
64	5	ACOGNO	New Orders for Consumer Goods
65*	5	AMDMNOx	New Orders for Durable Goods
66*	5	ANDENOx	New Orders for Nondefense Capital Goods
67*	5	AMDMUOx	Unfilled Orders for Durable Goods
68*	5	BUSINVx	Total Business Inventories
69*	2	ISRATIOx	Total Business: Inventories to Sales Ratio
130*	2	UMCSENTx	Consumer Sentiment Index

id	tcode	fred	description
Money and Credit			
70	6	M1SL	M1 Money Stock
71	6	M2SL	M2 Money Stock
72	5	M2REAL	Real M2 Money Stock
73	6	AMBSL	St. Louis Adjusted Monetary Base
74	6	TOTRESNS	Total Reserves of Depository Institutions
75	7	NONBORRES	Reserves Of Depository Institutions
76	6	BUSLOANS	Commercial and Industrial Loans
77	6	REALLN	Real Estate Loans at All Commercial Banks
78	6	NONREVSL	Total Nonrevolving Credit
79*	2	CONSPI	Nonrevolving consumer credit to Personal Income
131	6	MZMSL	MZM Money Stock
132	6	DTCOLNVHFNM	Consumer Motor Vehicle Loans Outstanding
133	6	DTCTHFNM	Total Consumer Loans and Leases Outstanding
134	6	INVEST	Securities in Bank Credit at All Commercial Banks
Interest Rates and Exchange Rates			
84	2	FEDFUNDS	Effective Federal Funds Rate
85*	2	CP3Mx	3-Month AA Financial Commercial Paper Rate
86	2	TB3MS	3-Month Treasury Bill:
87	2	TB6MS	6-Month Treasury Bill:
88	2	GS1	1-Year Treasury Rate
89	2	GS5	5-Year Treasury Rate
90	2	GS10	10-Year Treasury Rate
91	2	AAA	Moody's Seasoned Aaa Corporate Bond Yield
92	2	BAA	Moody's Seasoned Baa Corporate Bond Yield
93*	1	COMPAPFFx	3-Month Commercial Paper Minus FEDFUNDS
94	1	TB3SMFFM	3-Month Treasury C Minus FEDFUNDS
95	1	TB6SMFFM	6-Month Treasury C Minus FEDFUNDS
96	1	T1YFFM	1-Year Treasury C Minus FEDFUNDS
97	1	T5YFFM	5-Year Treasury C Minus FEDFUNDS
98	1	T10YFFM	10-Year Treasury C Minus FEDFUNDS
99	1	AAAFFM	Moody's Aaa Corporate Bond Minus FEDFUNDS
100	1	BAAFFM	Moody's Baa Corporate Bond Minus FEDFUNDS
101	5	TWEXMMTH	Trade Weighted U.S. Dollar Index: Major Currencies
102*	5	EXSZUSx	Switzerland / U.S. Foreign Exchange Rate
103*	5	EXJPUSx	Japan / U.S. Foreign Exchange Rate
104*	5	EXUSUKx	U.S. / U.K. Foreign Exchange Rate
105*	5	EXCAUSx	Canada / U.S. Foreign Exchange Rate

id	tcode	fred	description
Prices			
106	6	WPSFD49207	PPI: Finished Goods
107	6	WPSFD49502	PPI: Finished Consumer Goods
108	6	WPSID61	PPI: Intermediate Materials
109	6	WPSID62	PPI: Crude Materials
110*	6	OILPRICEx	Crude Oil, spliced WTI and Cushing
111	6	PPICMM	PPI: Metals and metal products:
112	1	NAPMPRI	ISM Manufacturing: Prices Index
113	6	CPIAUCSL	CPI : All Items
114	6	CPIAPPSL	CPI : Apparel
115	6	CPITRNSL	CPI : Transportation
116	6	CPIMEDSL	CPI : Medical Care
117	6	CUSR0000SAC	CPI : Commodities
118	6	CUUR0000SAD	CPI : Durables
119	6	CUSR0000SAS	CPI : Services
120	6	CPIULFSL	CPI : All Items Less Food
121	6	CUUR0000SA0L2	CPI : All items less shelter
122	6	CUSR0000SA0L5	CPI : All items less medical care
123	6	PCEPI	Personal Cons. Expend.: Chain Index
124	6	DDURRG3M086SBEA	Personal Cons. Exp: Durable goods
125	6	DNDGRG3M086SBEA	Personal Cons. Exp: Nondurable goods
126	6	DSERRG3M086SBEA	Personal Cons. Exp: Services
Stock Market			
80*	5	S&P 500	S&P's Common Stock Price Index: Composite
81*	5	S&P: indust	S&P's Common Stock Price Index: Industrials
82*	2	S&P div yield	S&P's Composite Common Stock: Dividend Yield
83*	5	S&P PE ratio	S&P's Composite Common Stock: Price-Earnings Ratio
135*	1	VXOCLSx	VXO